Exceptional service in the national interest

Sandia National Laboratories

SAND2020-2557PE

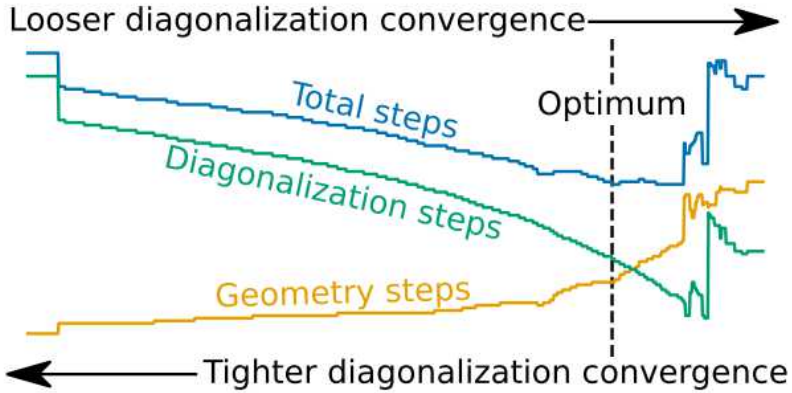

Automating Computational Catalysis Workflows

with Sella

Eric D. Hermes

2020-02-27

U.S. DEPARTMENT OF ENERGY

oratories is a multimission laboratory managed and operated by National Technology & Engineering Solutions of Sandia, neywell International Inc., for the U.S. Department of Energy's National Nuclear Security Administration under contract

Sandia National Laboratories

Introduction

Structure generation

- Background
- Catalyst model
- Developing a workflow

Sella paper

- Background
- Geometry updates
- Iterative diagonalization
- Hessian updates
- Results

Internal coordinates

- Background
- Geodesics
- Dealing with singularities
- Constraints

Exascale Catalytic Chemistry Project Overview

Goal: Develop an efficient, scalable, and fully open-source computational framework for automated reaction mechanism discovery and analysis of heterogeneous catalyst systems.

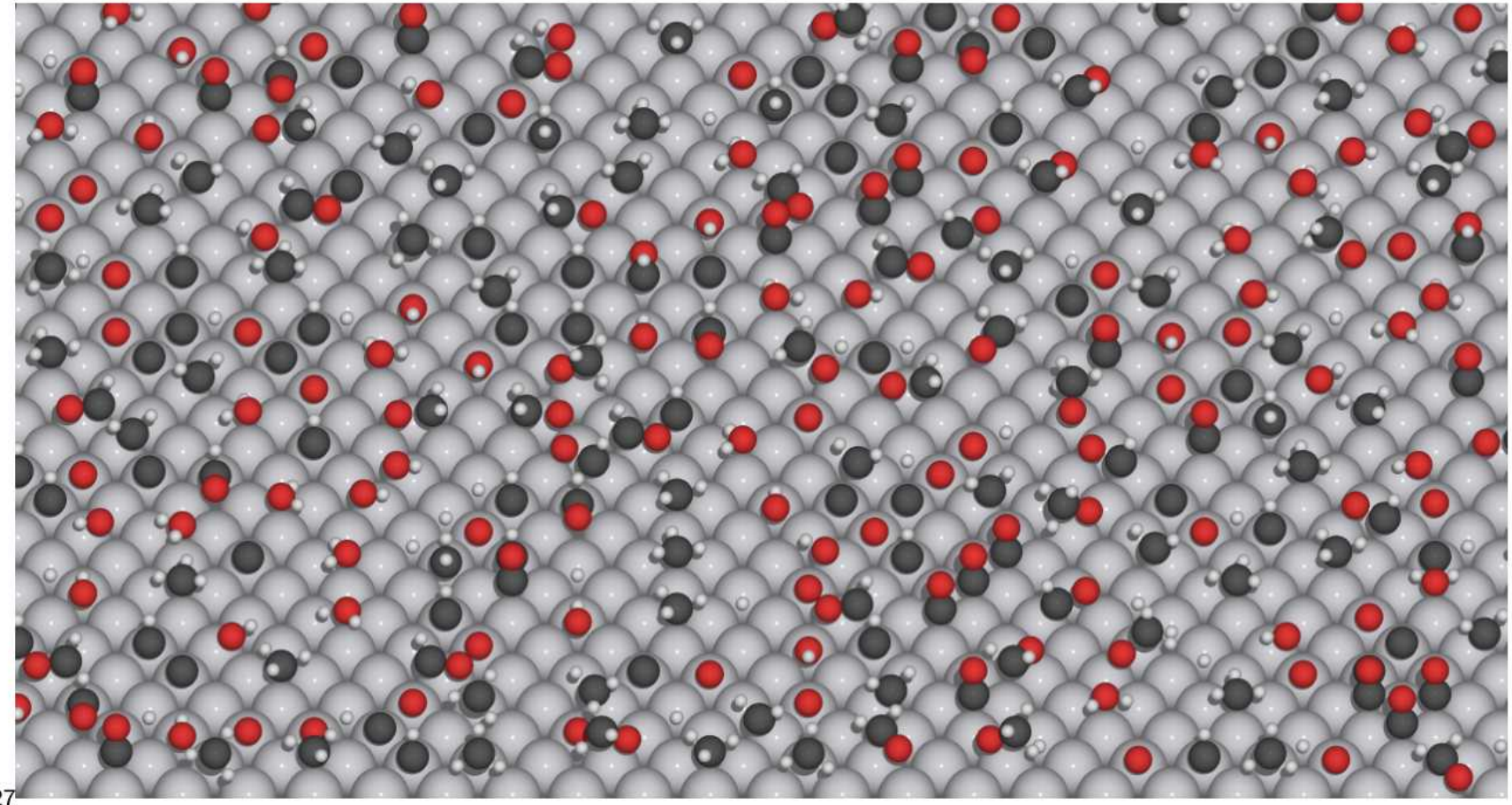

A recipe for *ab initio* microkinetic modeling

For the given catalyst, reactants, and products, propose a mechanism.

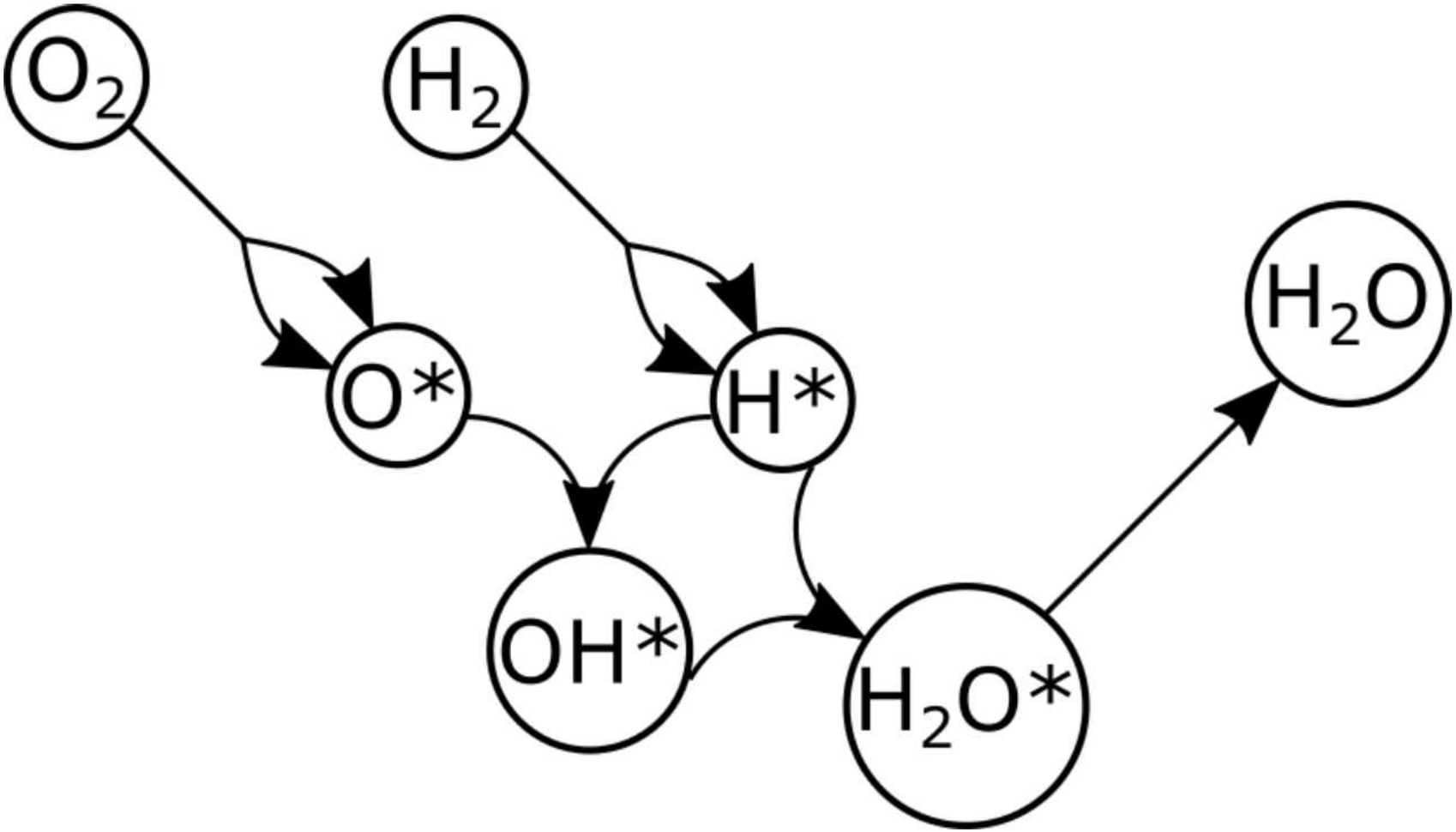

What if you get it wrong?

It's nearly impossible to tell that you *missed* crucial reactions and intermediates.

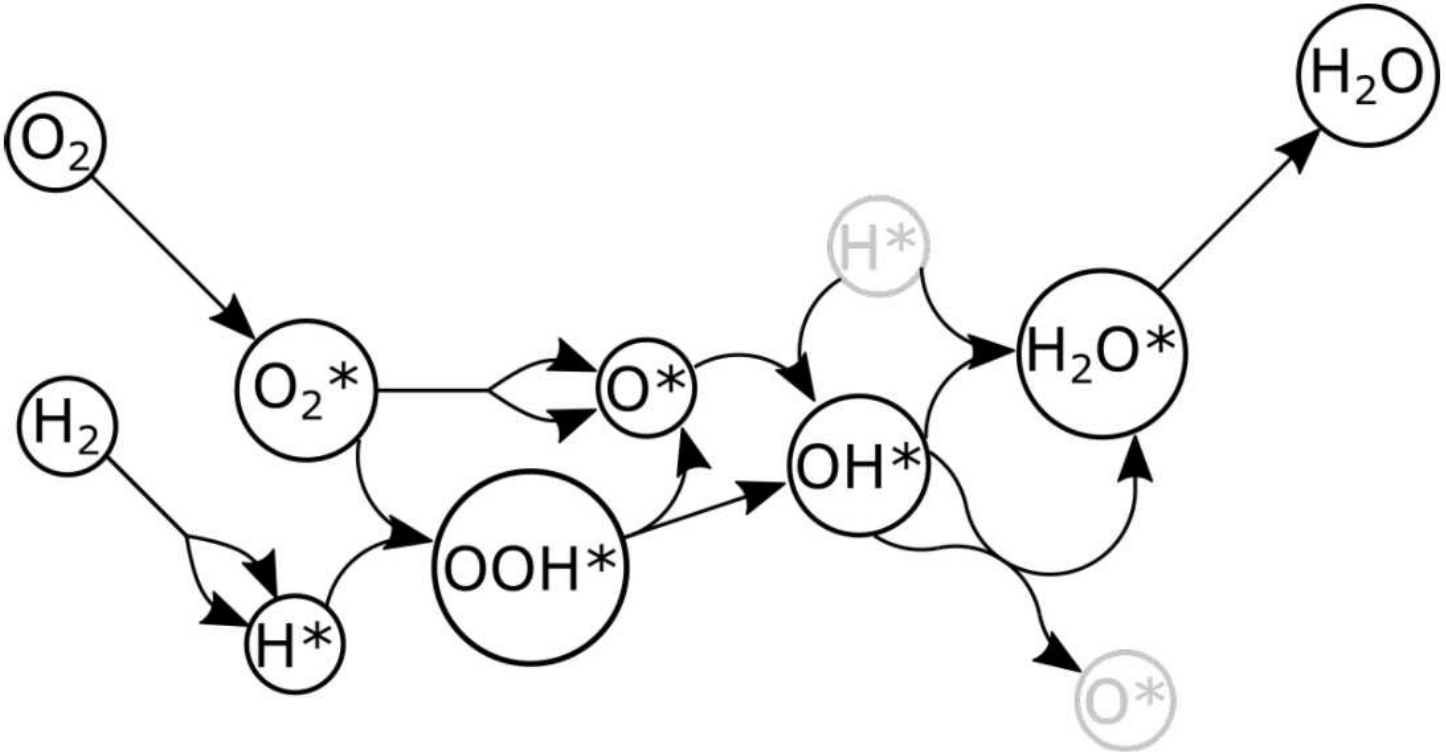

RMG[1] to the rescue

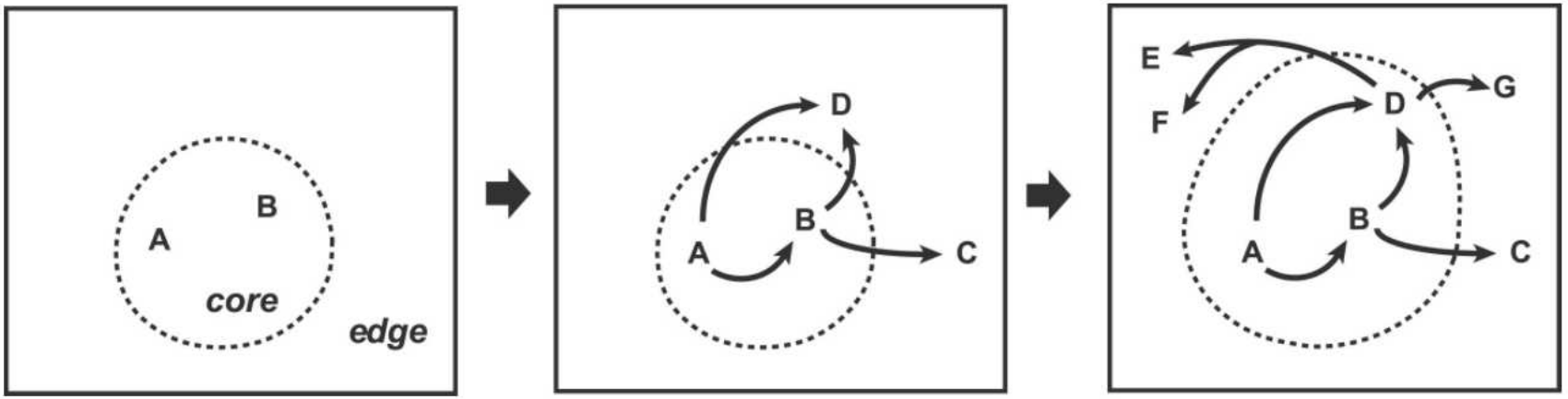

[1] Gao, C. W.; Allen, J. W.; Green, W. H.; West, R. H. *Computer Physics Communications* **2016**, *203*, 212–225

Updating RMG

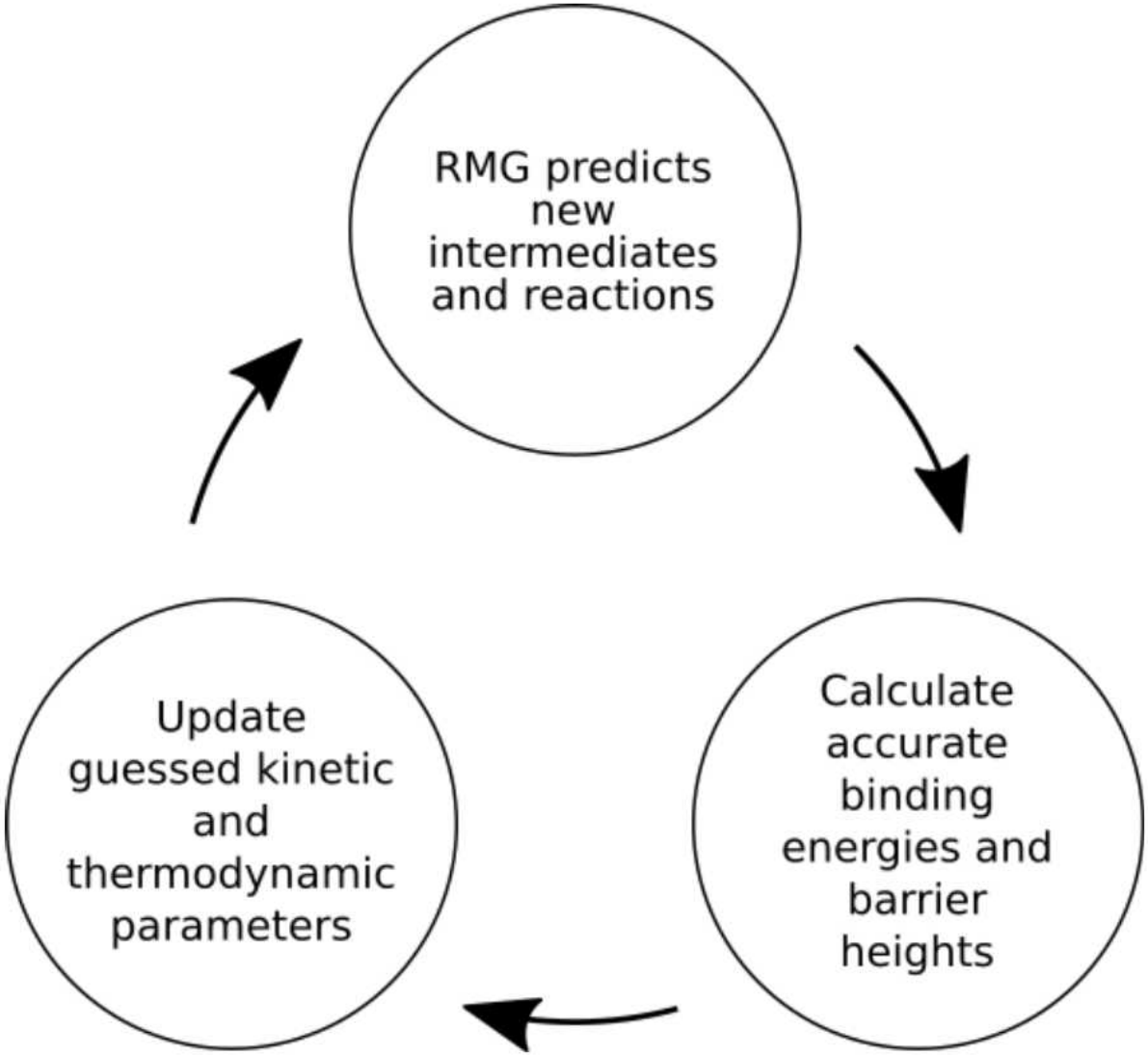

Updating RMG

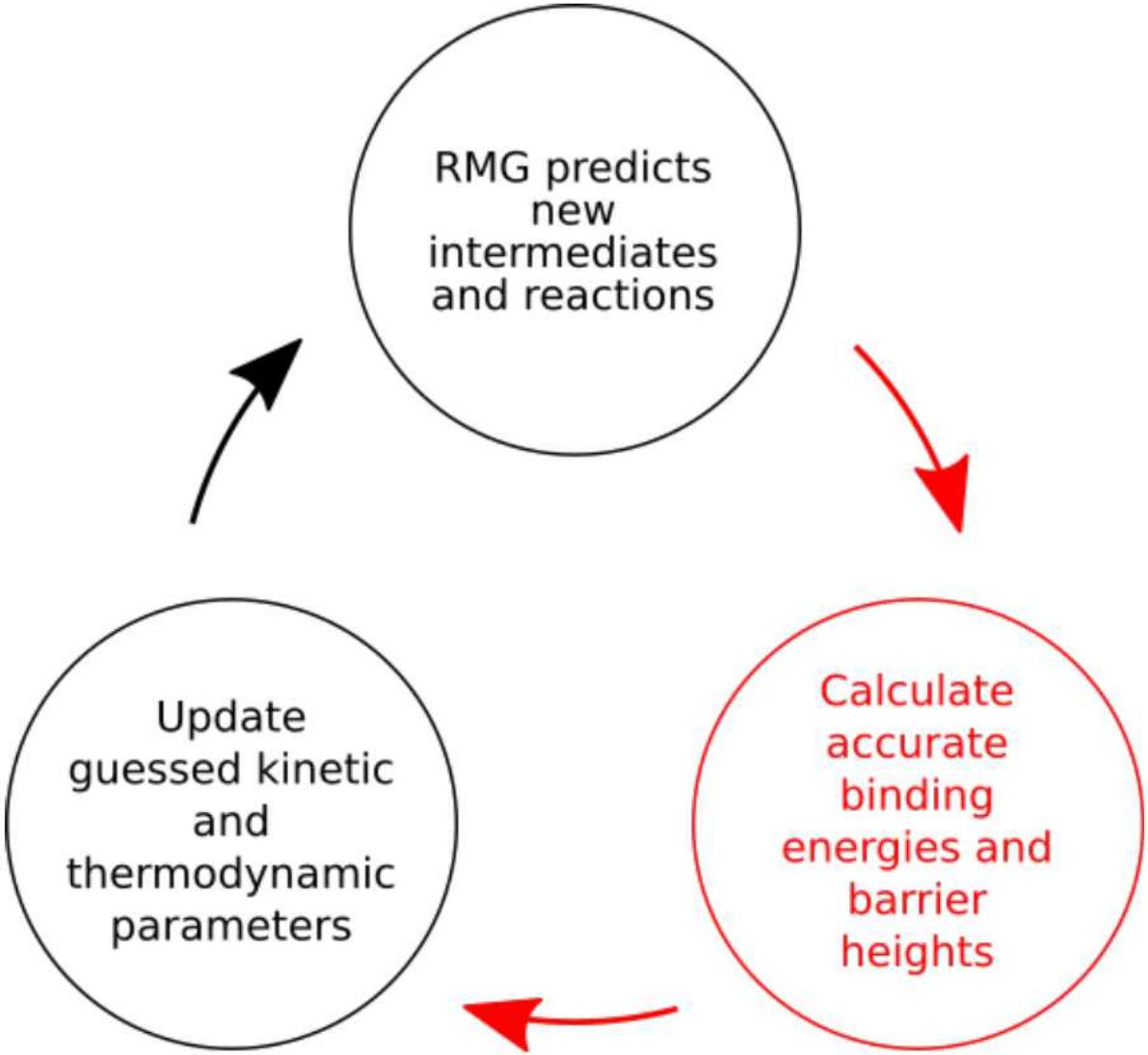

What RMG provides us

Gas-phase methyl radical:[1]

```
multiplicity 2
1 C u1 p0 c0 {2,S} {3,S} {4,S}
2 H u0 p0 c0 {1,S}
3 H u0 p0 c0 {1,S}
4 H u0 p0 c0 {1,S}
```

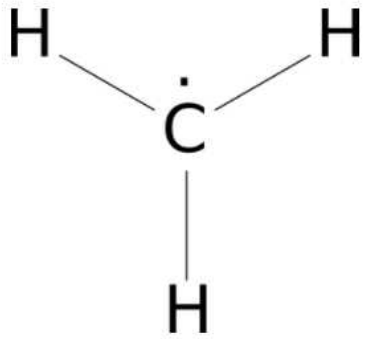

Methyl adsorbed to a surface:

```
multiplicity -187
1 C u0 p0 c0 {2,S} {3,S} {4,S} {5,S}
2 H u0 p0 c0 {1,S}
3 H u0 p0 c0 {1,S}
4 H u0 p0 c0 {1,S}
5 X u0 p0 c0 {1,S}
```

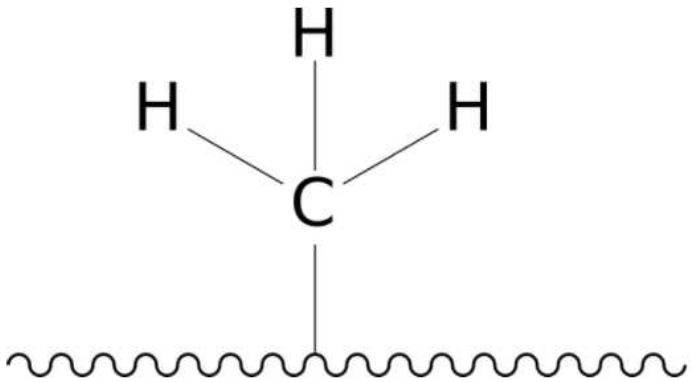

[1] Gao, C. W.; Allen, J. W.; Green, W. H.; West, R. H. *Computer Physics Communications* **2016**, *203*, 212–225

Catalytic reaction from RMG

```
- index: 6
  reaction: HOX(8) + CH2X(16) <=> OX(6) + CH3X(7)
  reaction_family: Surface_Abstraction
  reactant: |
      multiplicity -187
      1 *3 C u0 p0 c0 {2,S} {3,S} {4,S} {5,S}
      2 *4 H u0 p0 c0 {1,S}
      3    H u0 p0 c0 {1,S}
      4    H u0 p0 c0 {1,S}
      5 *5 X u0 p0 c0 {1,S}
      6 *1 O u0 p2 c0 {7,D}
      7 *2 X u0 p0 c0 {6,D}
  product: |
      multiplicity -187
      1 *3 C u0 p0 c0 {3,S} {4,S} {5,D}
      2 *4 H u0 p0 c0 {6,S}
      3    H u0 p0 c0 {1,S}
      4    H u0 p0 c0 {1,S}
      5 *5 X u0 p0 c0 {1,D}
      6 *1 O u0 p2 c0 {2,S} {7,S}
      7 *2 X u0 p0 c0 {6,S}
```

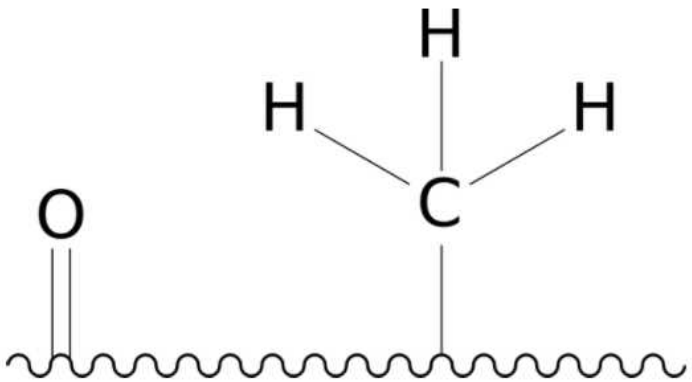

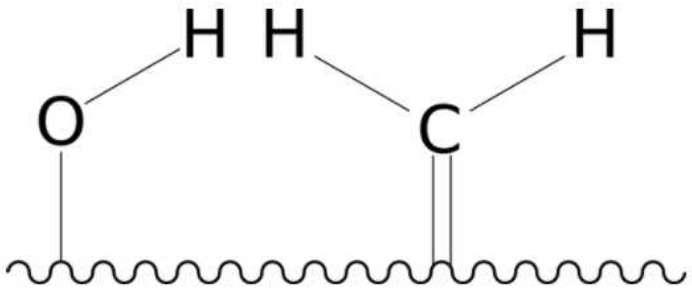

What do catalysts actually look like?[2]

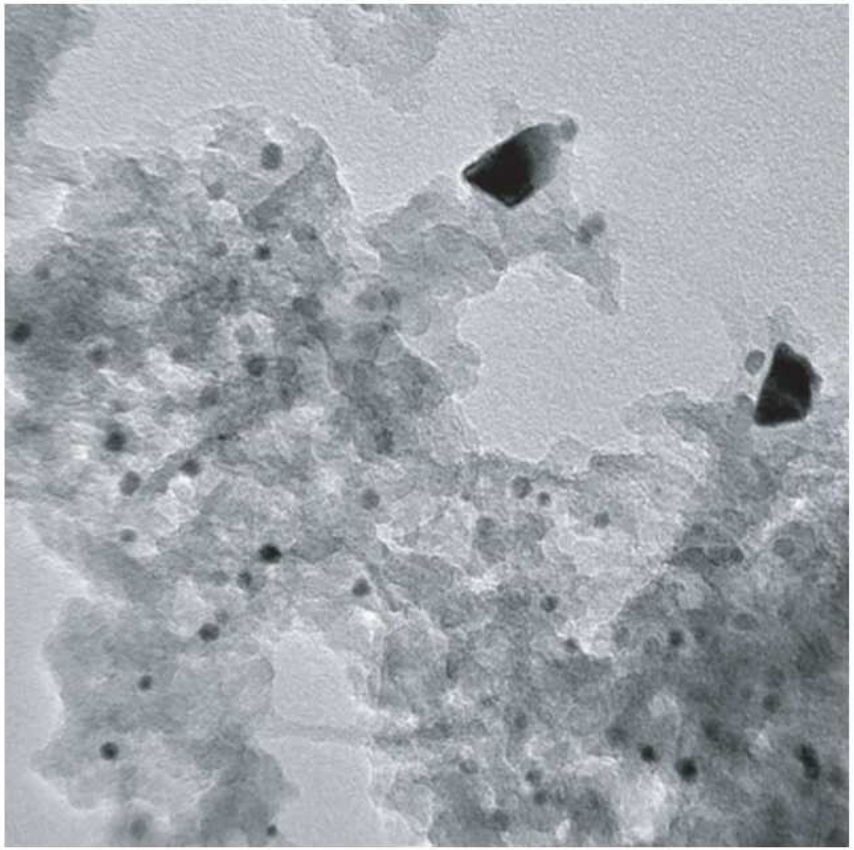

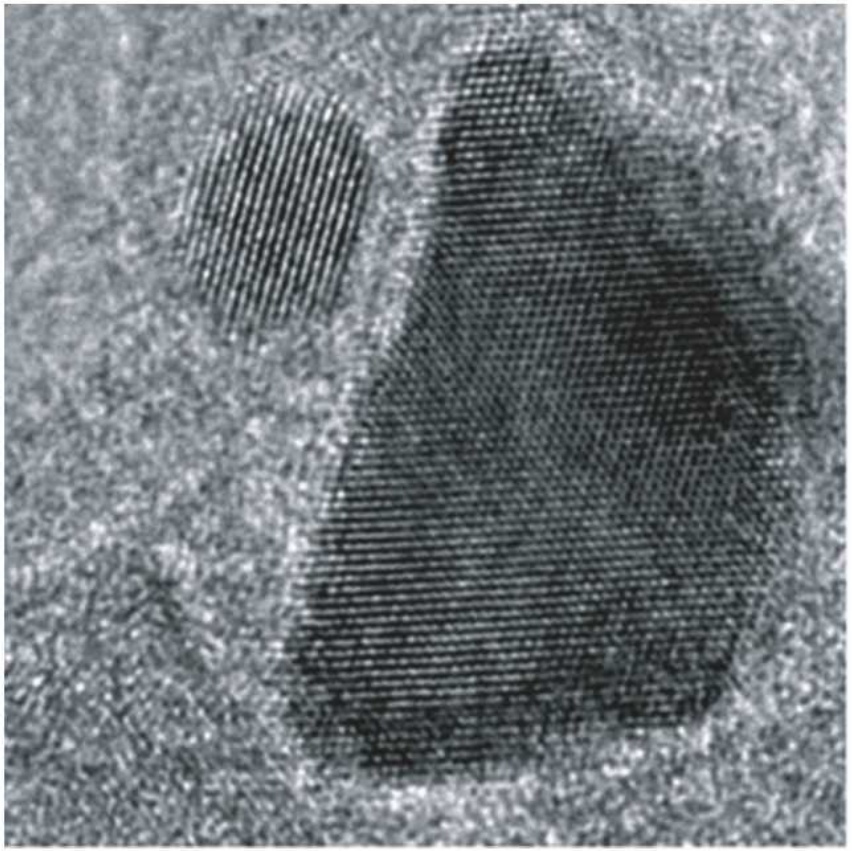

[2] Cao, A.; Veser, G. *Nature Materials* **2010**, *9*, 75–81

An idealized nanoparticle[3]

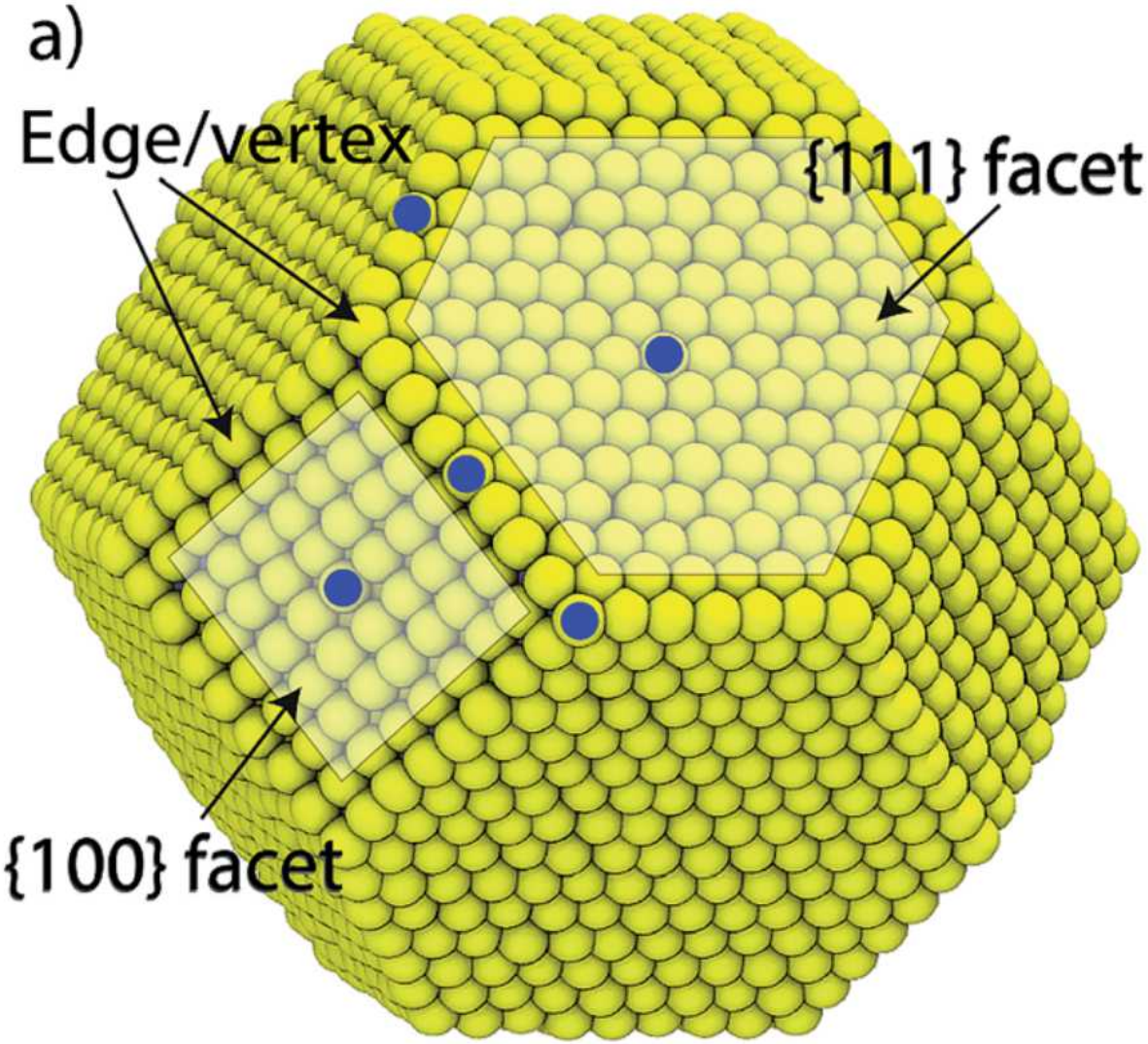

[3] Divi, S.; Chatterjee, A. *RSC Advances* **2018**, *8*, 10409–10424

Single crystal facets

FCC(100)

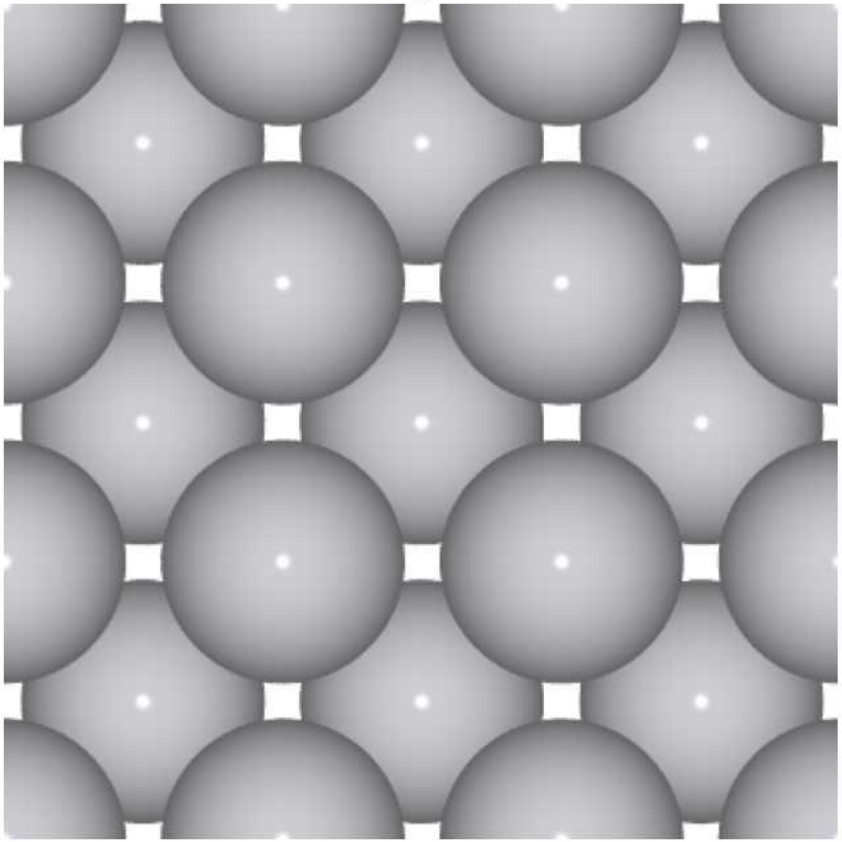

FCC(111)

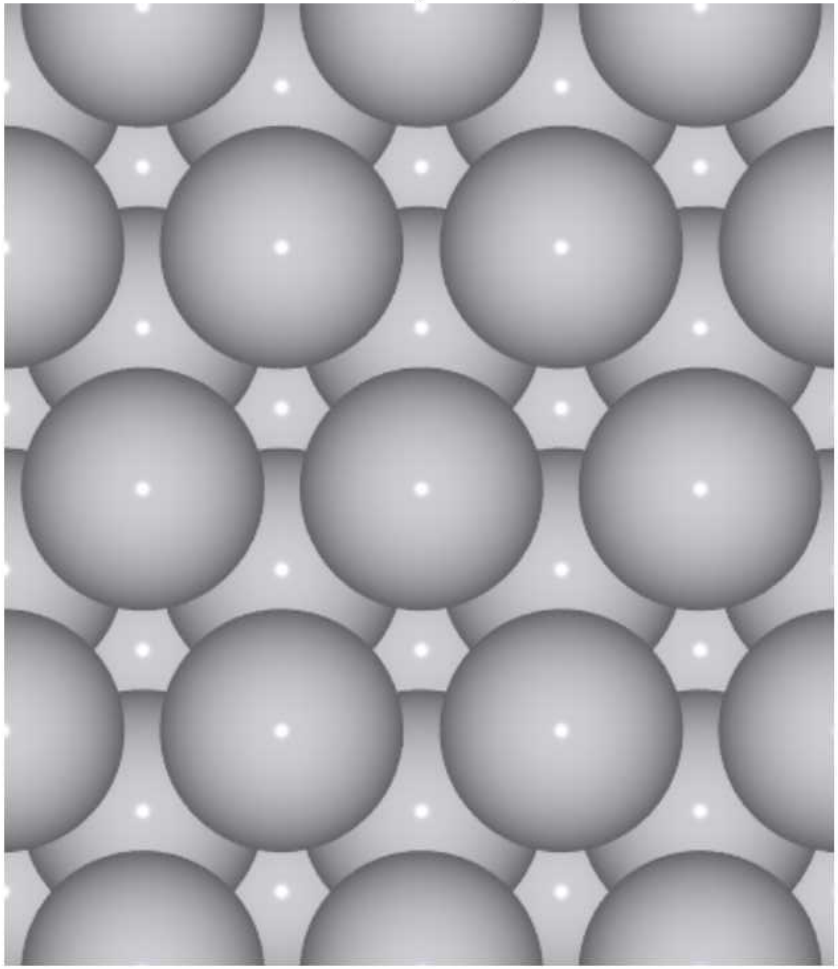

Slab model for DFT

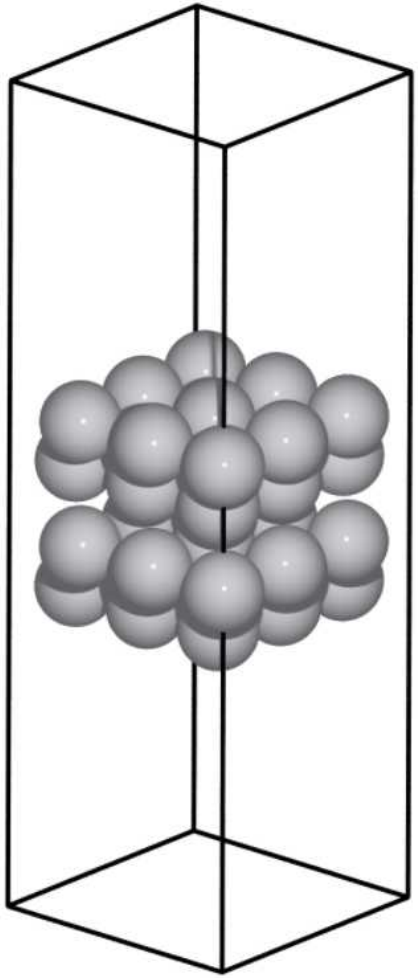

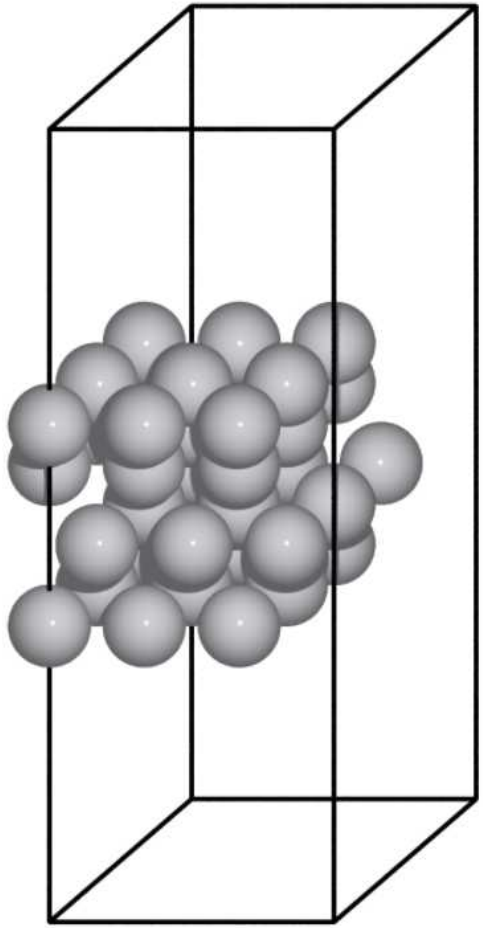

Single facet adsorption sites

FCC(100)

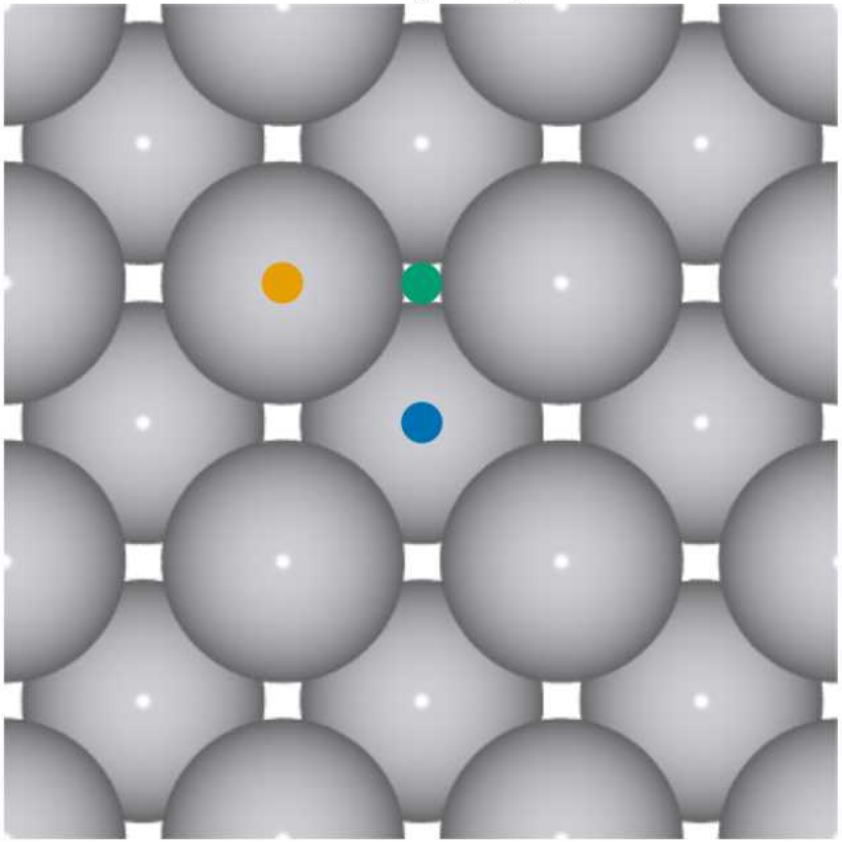

FCC(111)

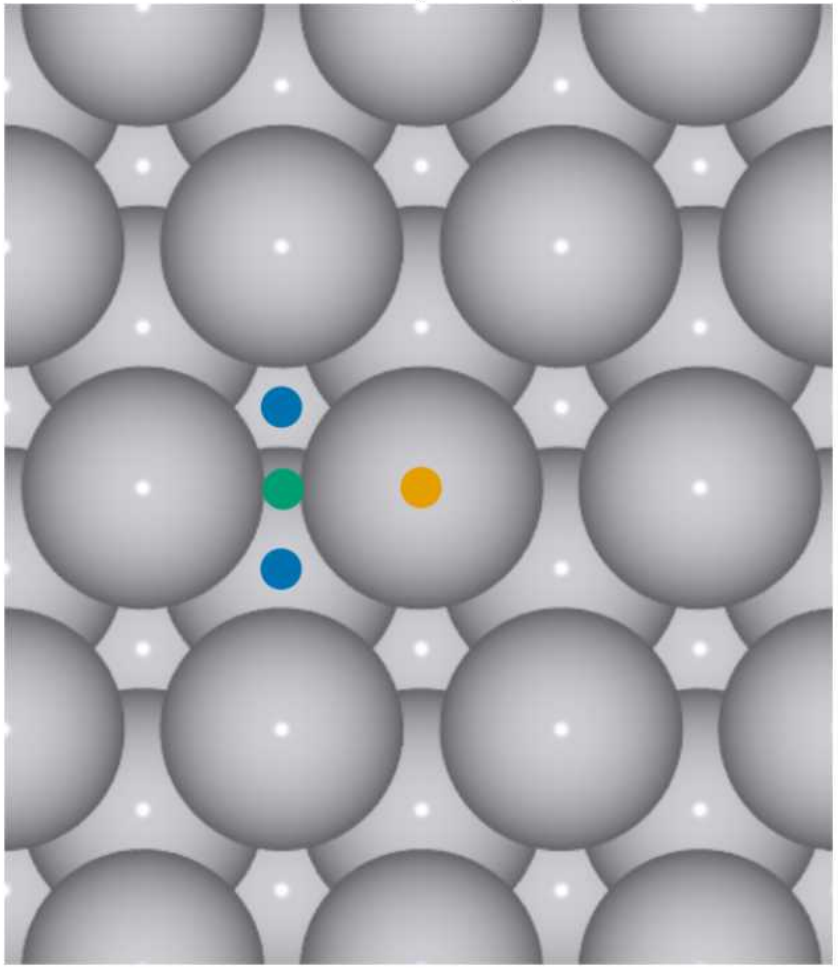

Hydrogen: initial structures

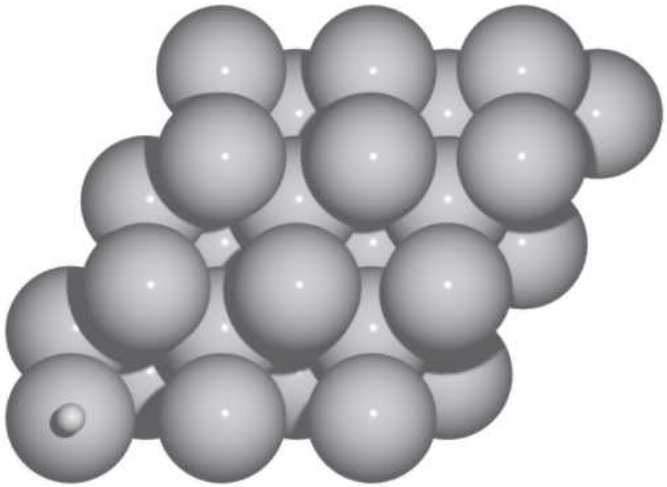

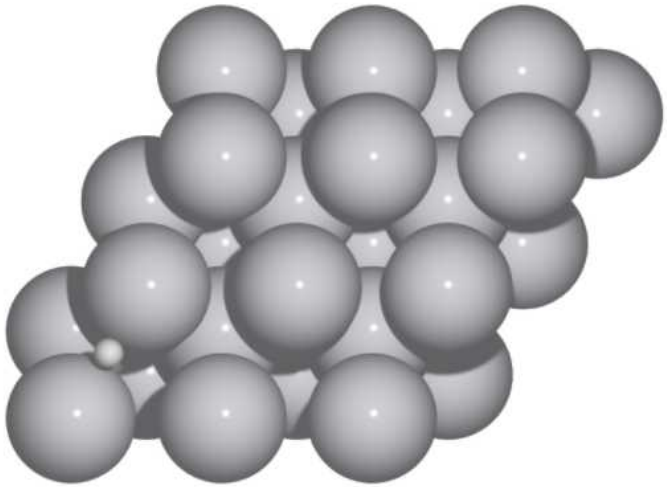

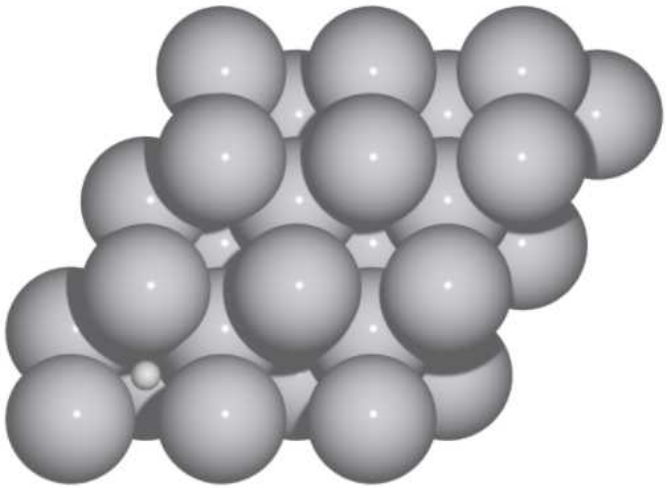

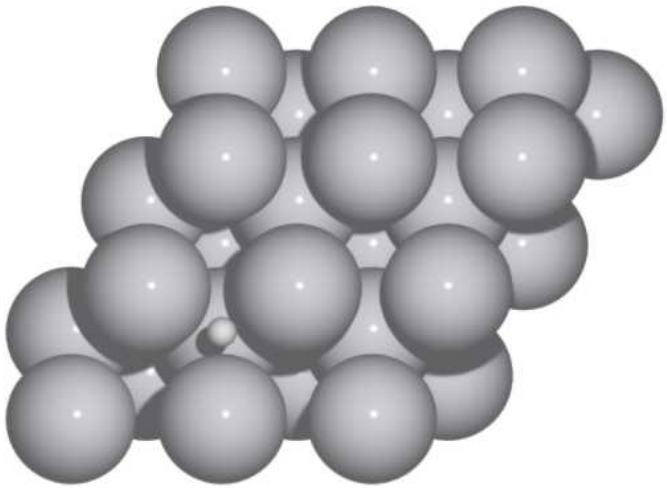

Hydrogen: final structures

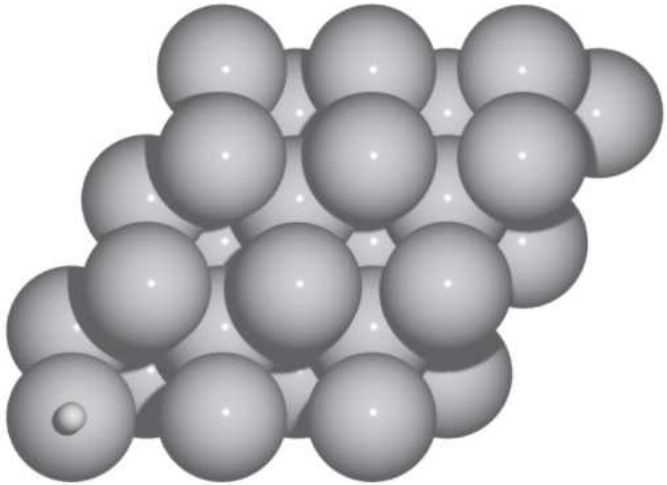

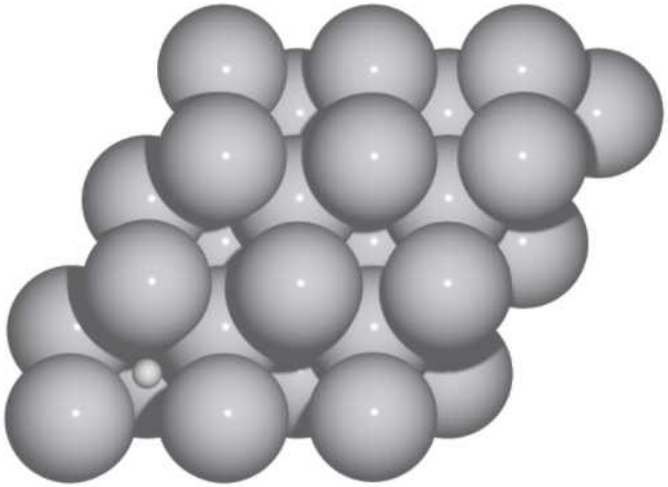

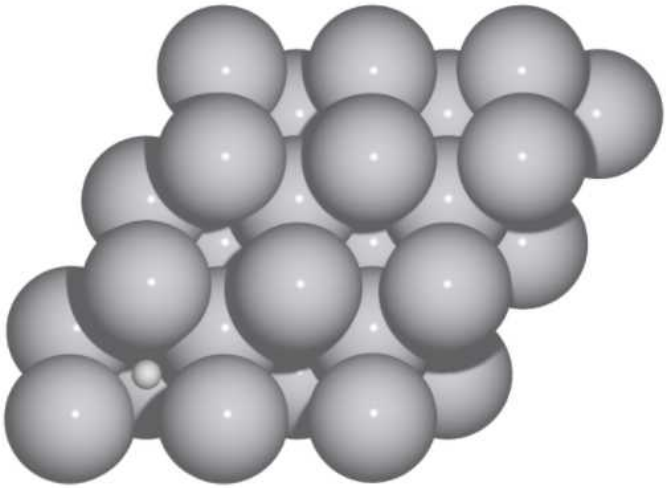

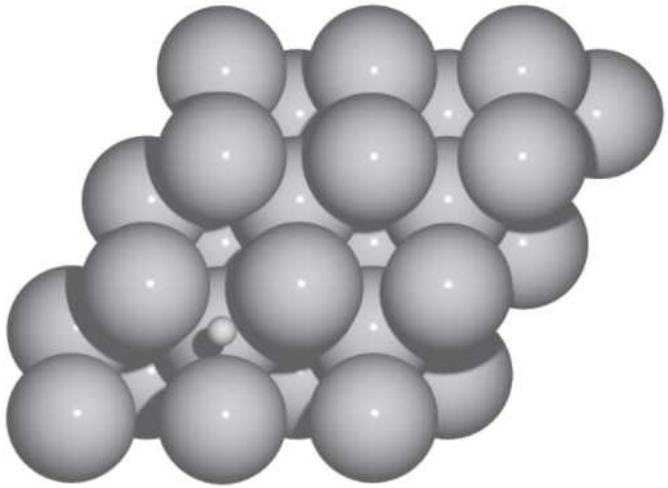

Finding symmetrically unique minima: XtalComp[4]

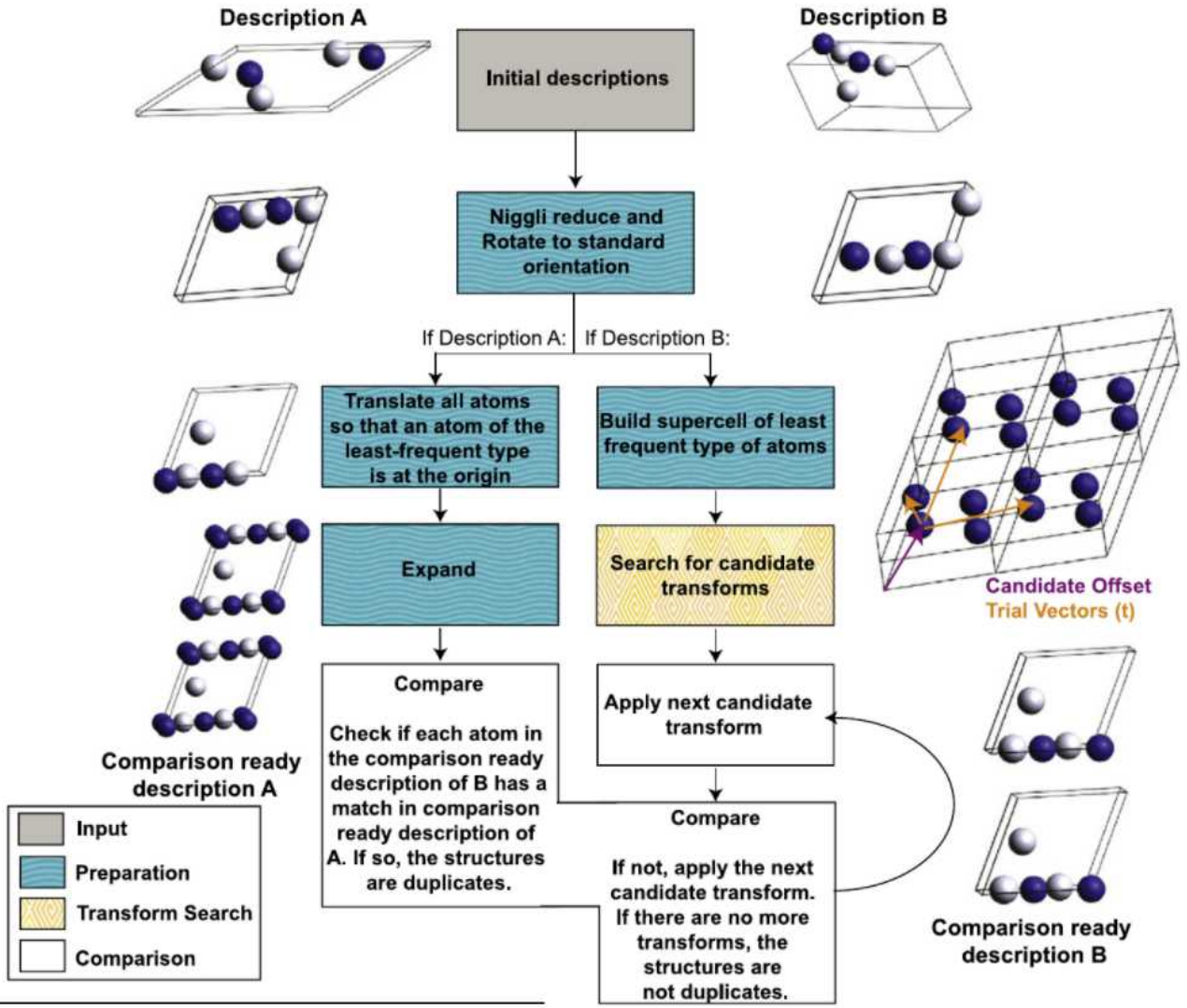

[4]Lonie, D. C.; Zurek, E. *Computer Physics Communications* **2012**, *183*, 690–697

Methlyene: initial structures

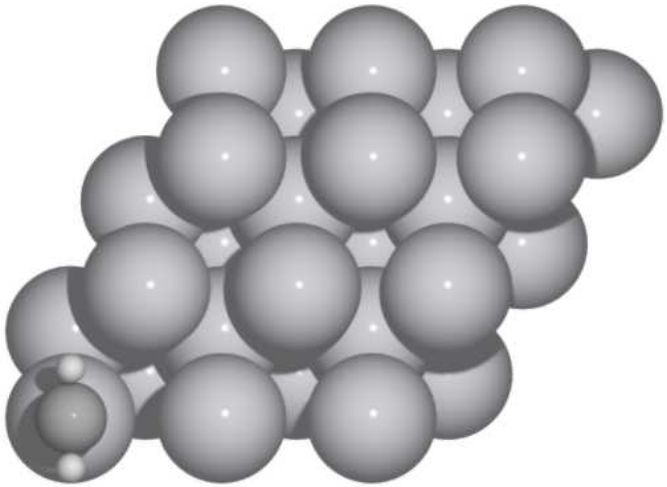

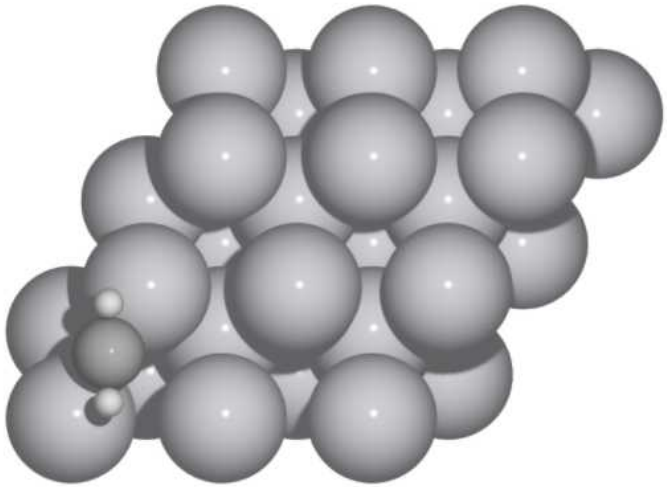

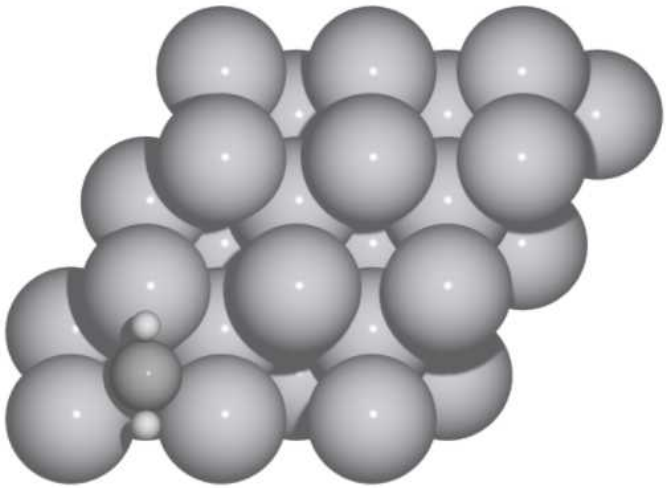

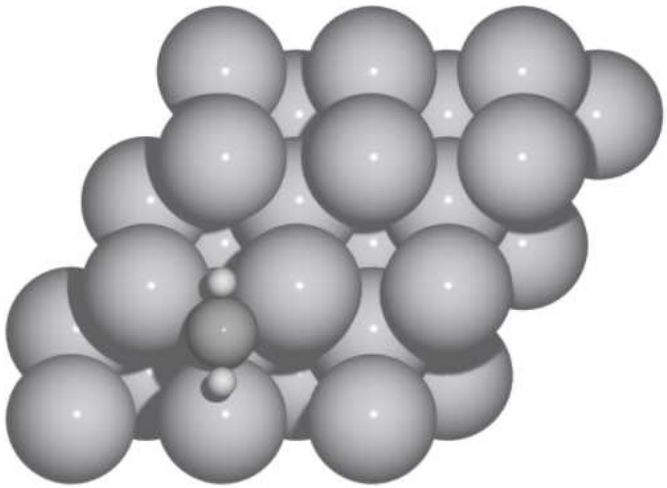

Methlyene: final structures

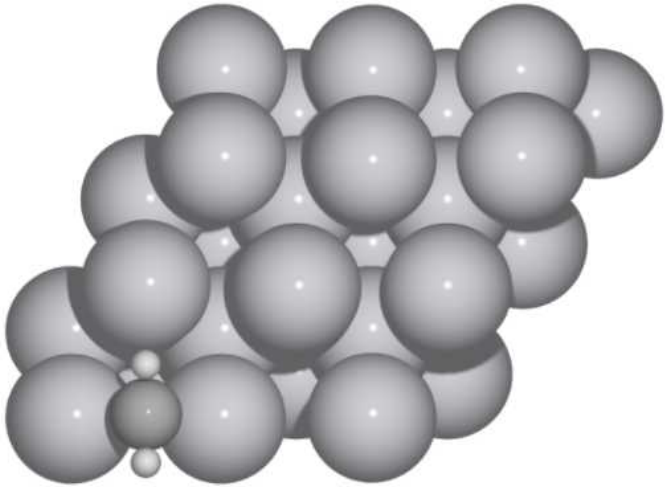

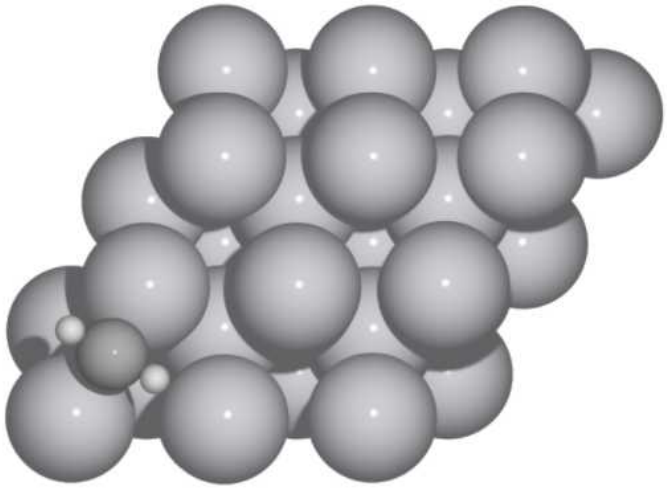

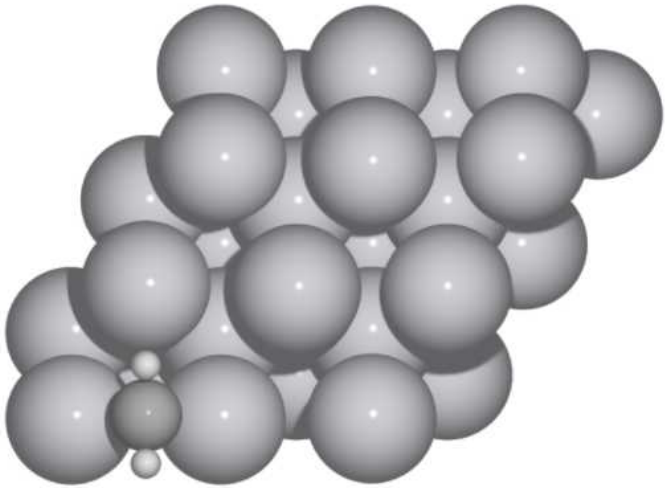

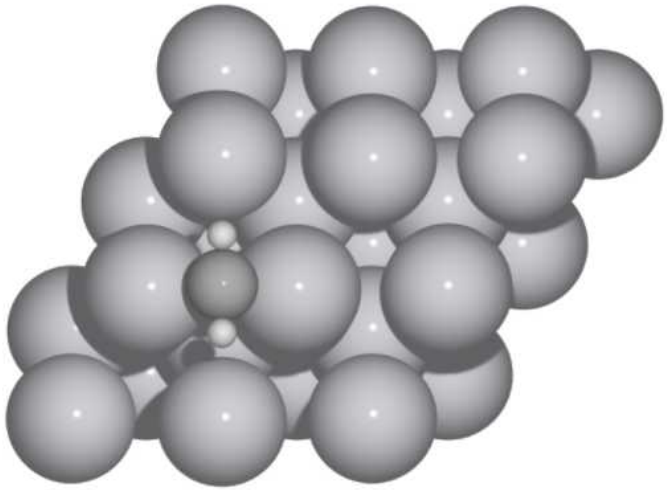

Methylene + H: initial structures

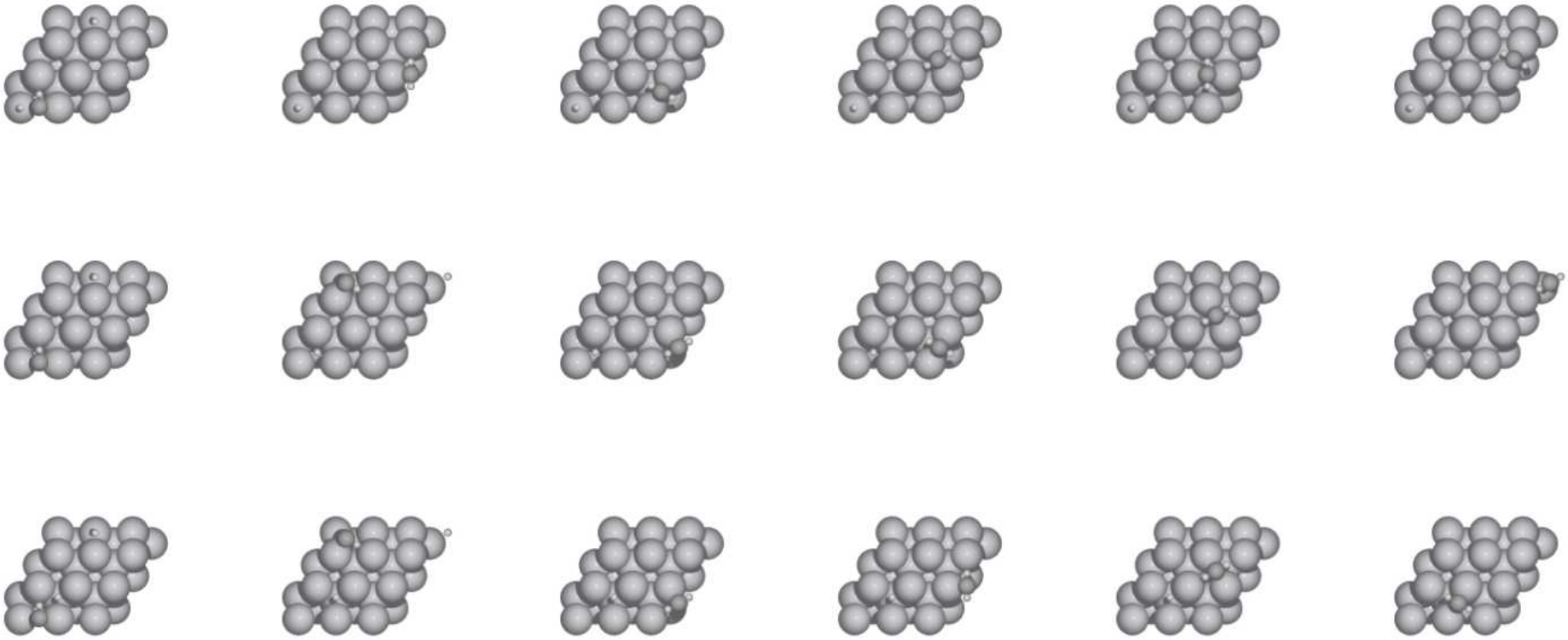

Methylene + H: final structures

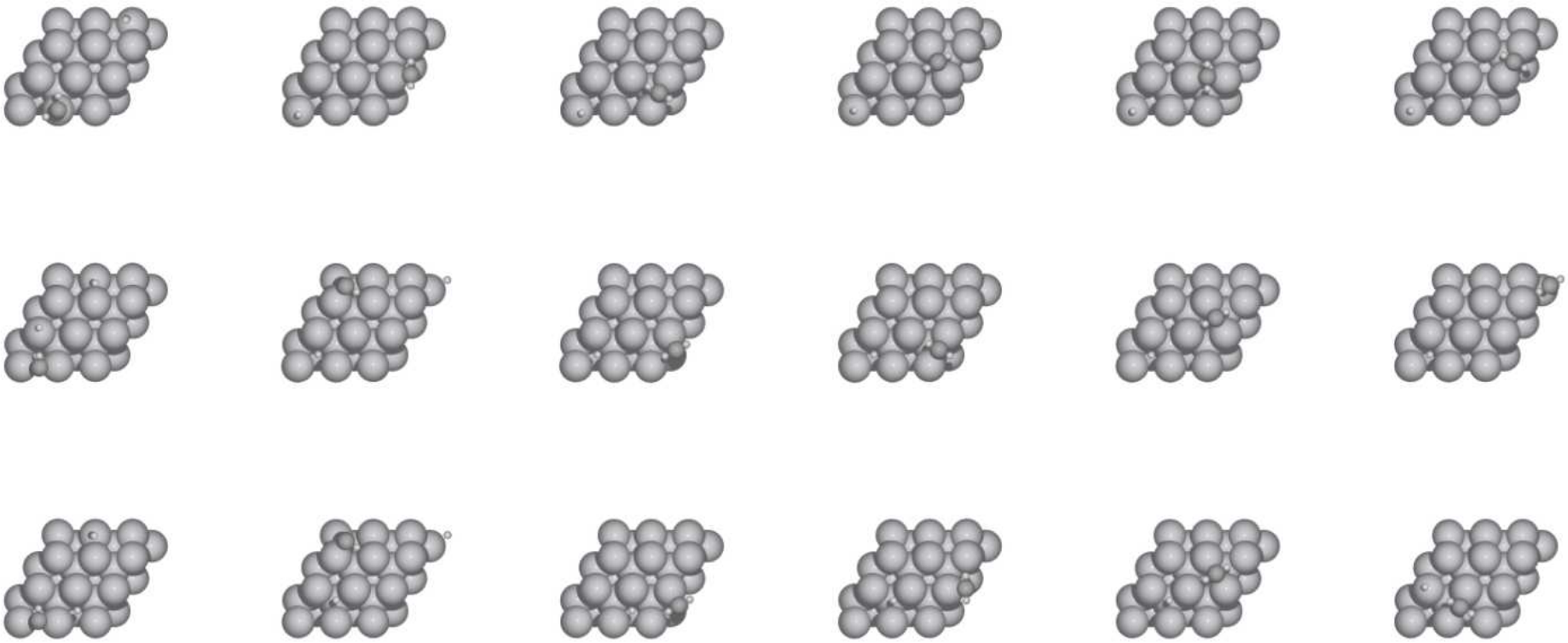

Higher index facets

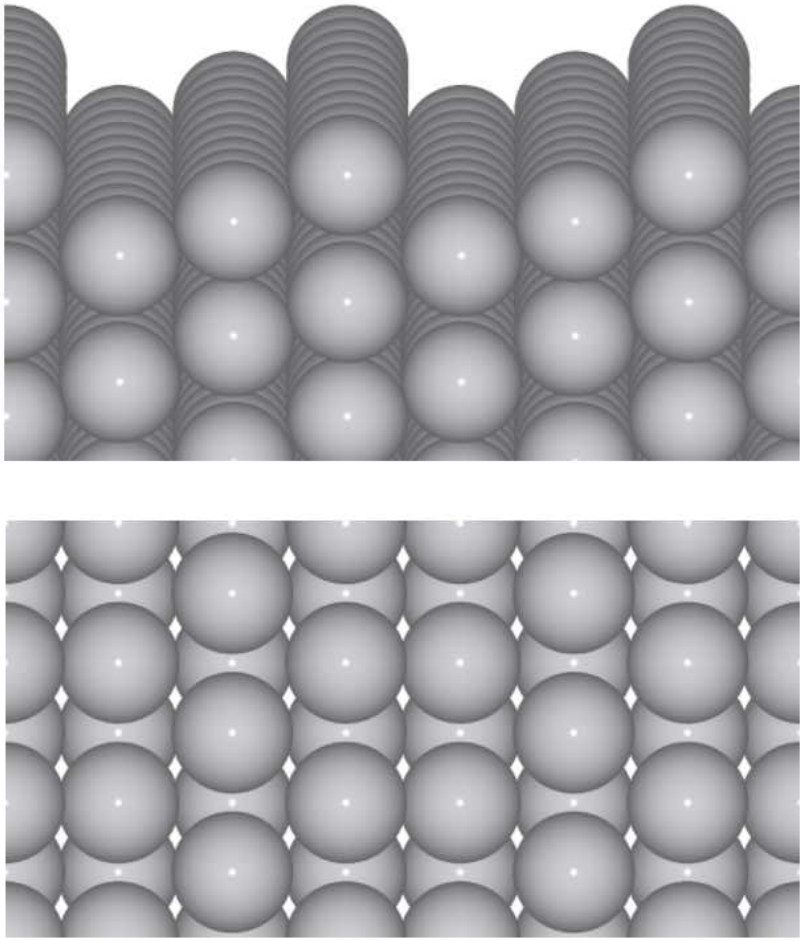

FCC(211) adsorption sites

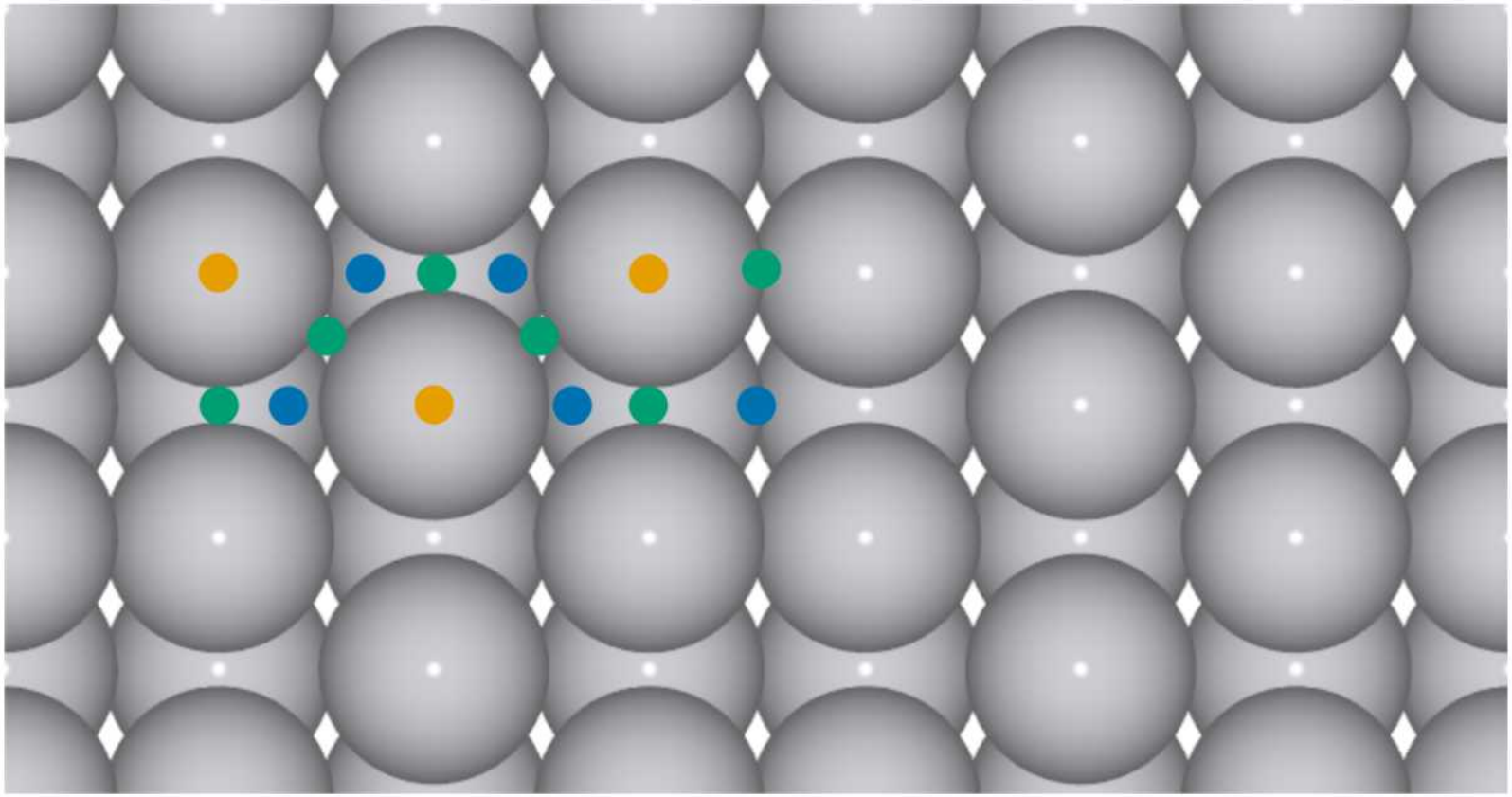

Sandia National Laboratories

Introduction

Structure generation
- Background
- Catalyst model
- Developing a workflow

Sella paper
- Background
- Geometry updates
- Iterative diagonalization
- Hessian updates
- Results

Internal coordinates
- Background
- Geodesics
- Dealing with singularities
- Constraints

Sella paper[5]

JCTC Journal of Chemical Theory and Computation

Article

Cite This: J. Chem. Theory Comput. 2019, 15, 6536–6549

pubs.acs.org/JCTC

Accelerated Saddle Point Refinement through Full Exploitation of Partial Hessian Diagonalization

Eric D. Hermes, Khachik Sargsyan, Habib N. Najm, and Judit Zádor*

Combustion Research Facility, Sandia National Laboratories, Livermore, California 94551-0969, United States

Supporting Information

ABSTRACT: Identification and refinement of first order saddle point (FOSP) structures on the potential energy surface (PES) of chemical systems is a computational bottleneck in the characterization of reaction pathways. Leading FOSP refinement strategies for modestly sized molecular systems require calculation of the full Hessian matrix, which is not feasible for larger systems such as those encountered in heterogeneous catalysis. For these systems, the standard approach to FOSP refinement involves iterative diagonalization of the Hessian, but this comes at the cost of longer refinement trajectories due to the lack of accurate curvature information. We present a method for incorporating information obtained by an iterative diagonalization algorithm into the construction of an approximate Hessian matrix that accelerates FOSP refinement. We measure the performance of our method with two established FOSP refinement benchmarks and find a 50% reduction on average in the number of gradient evaluations required to converge to a FOSP for one benchmark and a 25% reduction on average for the second benchmark.

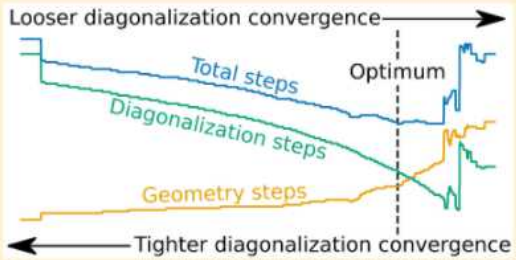

[5]Hermes, E. D.; Sargsyan, K.; Najm, H. N.; Zádor, J. *Journal of Chemical Theory and Computation* **2019**, *15*, 6536–6549

PES and optimization[6]

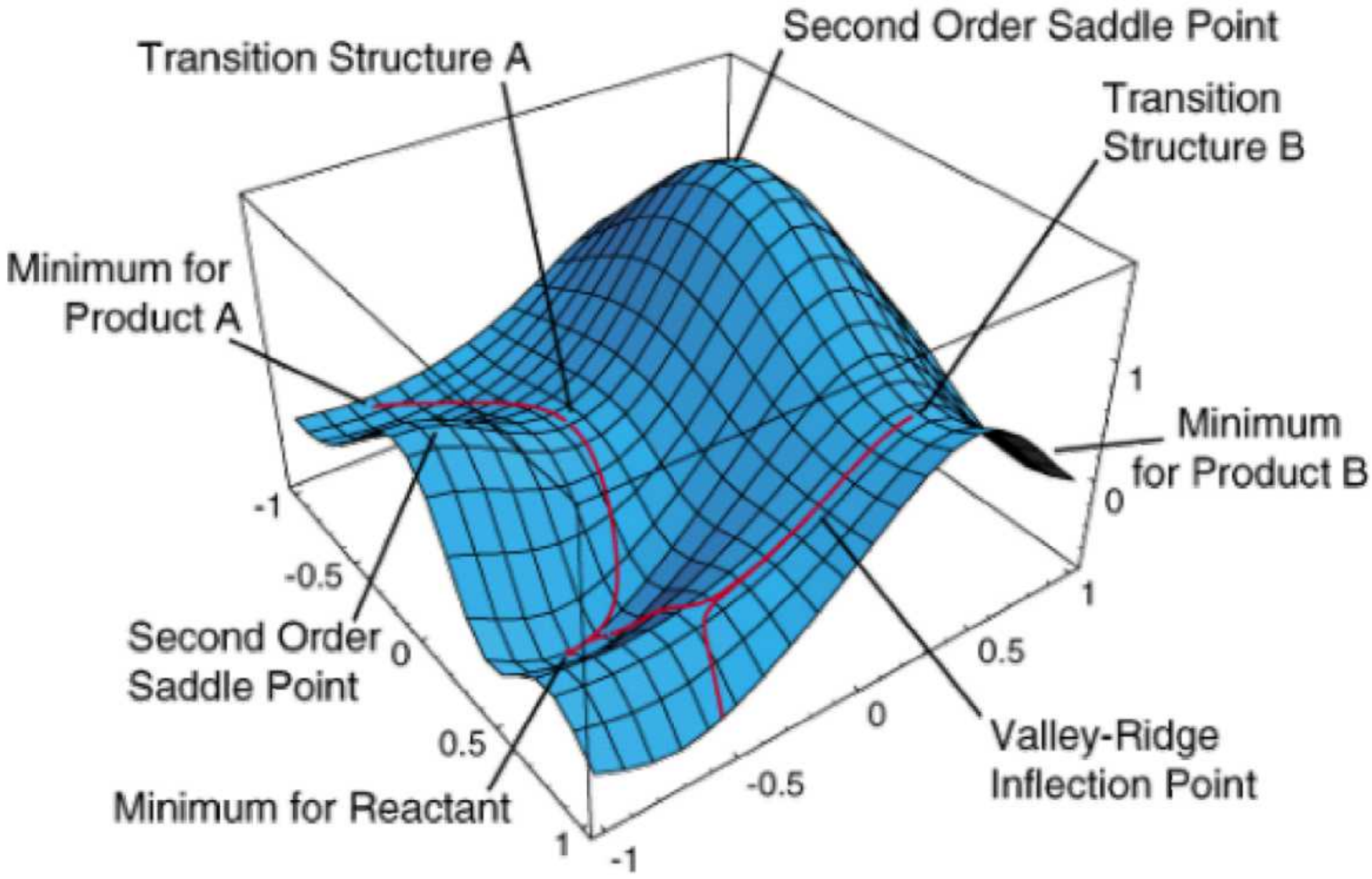

[6] Schlegel, H. B. *Journal of Computational Chemistry* **1982**, *3*, 214–218

Established FOSP refinement procedures

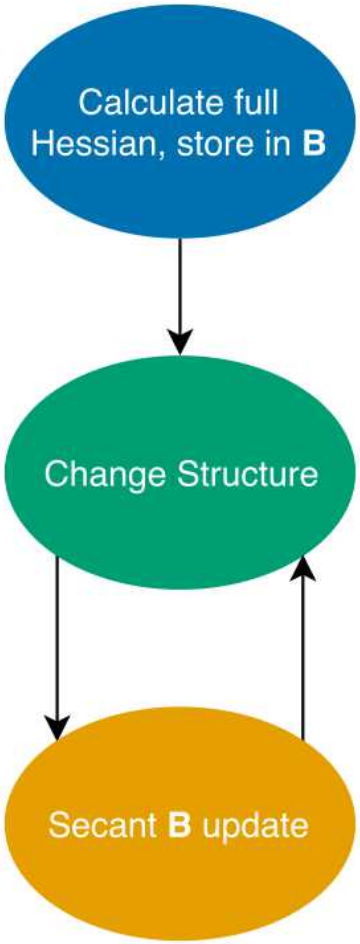

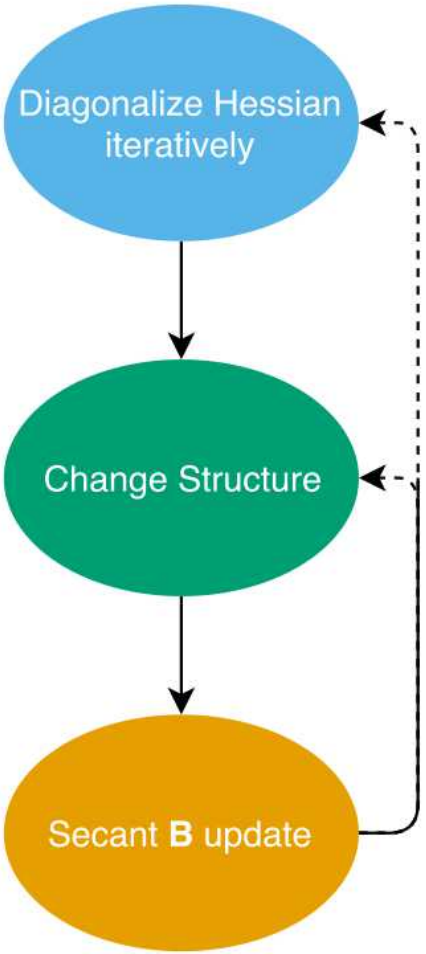

Sella's procedure

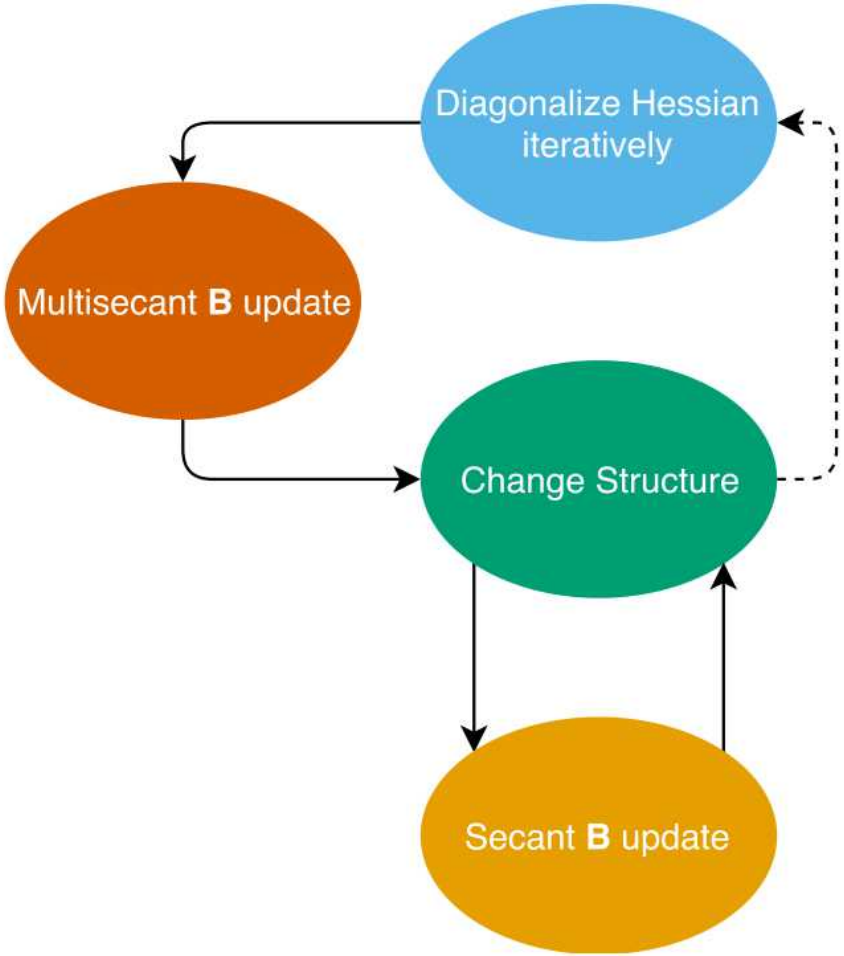

Geometry optimization

Expand the potential energy surface (PES) to second order around the current point $\mathbf{x}$:

$$\tilde{\epsilon}(\mathbf{x}+\mathbf{s}) = \epsilon(\mathbf{x}) + \mathbf{g}(\mathbf{x})^T\mathbf{s} + \frac{1}{2}\mathbf{s}^T\mathbf{H}(\mathbf{x})\mathbf{s}$$

Newton-Raphson: solve for $\frac{d\tilde{\epsilon}}{d\mathbf{s}} = \mathbf{0}$.
Quasi-Newton: replace $\mathbf{H}(\mathbf{x})$ with an approximation, $\mathbf{B}$.
Restricted step: add the constraint that $\|\mathbf{s}\|_2 \leq \delta$.

Rational function optimization

RFO: minimize the weighted energy function:

$$\mu = \frac{\mathbf{g}^T\mathbf{s} + \frac{1}{2}\mathbf{s}^T\mathbf{B}\mathbf{s}}{1 + \mathbf{s}^T\mathbf{W}\mathbf{s}}$$

This can be rearranged to:

$$\begin{bmatrix}\mathbf{s}^T & 1\end{bmatrix}\begin{bmatrix}\mathbf{B} & \mathbf{g}\\ \mathbf{g}^T & 0\end{bmatrix}\begin{bmatrix}\mathbf{s}\\ 1\end{bmatrix} = 2\mu\begin{bmatrix}\mathbf{s}^T & 1\end{bmatrix}\begin{bmatrix}\mathbf{W} & \mathbf{0}\\ \mathbf{0}^T & 1\end{bmatrix}\begin{bmatrix}\mathbf{s}\\ 1\end{bmatrix}$$

The stationary points of this function are given by:

$$\begin{bmatrix}\mathbf{B} & \mathbf{g}\\ \mathbf{g}^T & 0\end{bmatrix}\begin{bmatrix}\mathbf{s}\\ 1\end{bmatrix} = 2\mu\begin{bmatrix}\mathbf{W} & \mathbf{0}\\ \mathbf{0}^T & 1\end{bmatrix}\begin{bmatrix}\mathbf{s}\\ 1\end{bmatrix}$$

Partitioned rational function optimization

Split the full optimization space into a "maximization" subspace $\tilde{\mathbf{V}}^{(\max)}$ and a "minimization" subspace $\tilde{\mathbf{V}}^{(\min)}$ where $\begin{bmatrix}\tilde{\mathbf{V}}^{(\max)} & \tilde{\mathbf{V}}^{(\min)}\end{bmatrix}$ are the eigenvectors of $\mathbf{B}$. Then write two RFO equations:

$$\begin{bmatrix}\mathbf{B}^{(\max)} & \mathbf{g}^{(\max)} \\ \mathbf{g}^{(\max)T} & 0\end{bmatrix}\begin{bmatrix}\mathbf{s}^{(\max)} \\ 1\end{bmatrix} = 2\mu^{(\max)}\begin{bmatrix}\mathbf{W}^{(\max)} & \mathbf{0} \\ \mathbf{0}^T & 1\end{bmatrix}\begin{bmatrix}\mathbf{s}^{(\max)} \\ 1\end{bmatrix}$$

$$\begin{bmatrix}\mathbf{B}^{(\min)} & \mathbf{g}^{(\min)} \\ \mathbf{g}^{(\min)T} & 0\end{bmatrix}\begin{bmatrix}\mathbf{s}^{(\min)} \\ 1\end{bmatrix} = 2\mu^{(\min)}\begin{bmatrix}\mathbf{W}^{(\min)} & \mathbf{0} \\ \mathbf{0}^T & 1\end{bmatrix}\begin{bmatrix}\mathbf{s}^{(\min)} \\ 1\end{bmatrix}$$

- $\mathbf{B}^{(\max)} = \tilde{\mathbf{V}}^{(\max)T}\mathbf{B}\tilde{\mathbf{V}}^{(\max)}$
- $\mathbf{g}^{(\max)} = \tilde{\mathbf{V}}^{(\max)T}\mathbf{g}$
- $\mathbf{W}^{(\max)} = \tilde{\mathbf{V}}^{(\max)T}\mathbf{W}\tilde{\mathbf{V}}^{(\max)}$
- $\mathbf{B}^{(\min)}$, $\mathbf{g}^{(\min)}$, and $\mathbf{W}^{(\min)}$ are defined analogously.

Then $\mathbf{s} = \tilde{\mathbf{V}}^{(\max)}\mathbf{s}^{(\max)} + \tilde{\mathbf{V}}^{(\min)}\mathbf{s}^{(\min)}$.

Iterative diagonalization

Hessian-vector products can be approximated by finite difference:

$$\mathbf{Hs} \approx \frac{\mathbf{g}(\mathbf{x} + \eta\mathbf{s}) - \mathbf{g}(\mathbf{x})}{\eta}$$

Given an orthonormal matrix of displacement vectors $\mathbf{S}$ and the corresponding approximate Hessian-vector products $\mathbf{Y} \approx \mathbf{HS}$:

1. Calculate eigenvalues θ_j and eigenvectors $\mathbf{c}_j$ of $\mathbf{S}^T\mathbf{Y}$
2. Calculate Ritz vector $\mathbf{x}_j = \mathbf{S}\mathbf{c}_j$ and its residual $\mathbf{r}_j = \mathbf{Y}\mathbf{c}_j - \theta_j\mathbf{x}_j$ for the desired eigenpair
3. Is $\|\mathbf{r}_j\|_2$ small relative to θ_j? If so, end diagonalization.
4. Otherwise, expand $\mathbf{S}$ with a new vector $\mathbf{s}$, expand $\mathbf{Y}$ with $\mathbf{Hs}$, and go back to step 1.

Approximate Hessian updates

Given a previous approximate Hessian $\mathbf{B}$ and new curvature information in $\mathbf{S}$ and $\mathbf{Y}$, how do we construct a new and improved approximate Hessian? Multi-secant Greenstadt provides a general formula:

$$\mathbf{B}^{+} = \mathbf{B} + \mathbf{U}\mathbf{J}^{T} + \mathbf{J}\mathbf{U}^{T} - \mathbf{U}\mathbf{J}^{T}\mathbf{S}\mathbf{U}^{T}$$
$$\mathbf{J} = \mathbf{Y} - \mathbf{B}\mathbf{S}$$
$$\mathbf{U} = \mathbf{M}\mathbf{S}\left[\mathbf{S}^{T}\mathbf{M}\mathbf{S}\right]^{-1}$$

Different updates are obtained for different choices of $\mathbf{M}$. For example:

- $\mathbf{M}^{\mathrm{PSB}} = \mathbf{I}$
- $\mathbf{M}^{\mathrm{MS}} = \mathbf{B}^{+} - \mathbf{B}$
- $\mathbf{M}^{\mathrm{BFGS}} = \frac{\sqrt{\mathbf{S}^{T}\mathbf{B}\mathbf{S}}\mathbf{B}^{+} + \sqrt{\mathbf{Y}^{T}\mathbf{S}}\mathbf{B}}{\sqrt{\mathbf{Y}^{T}\mathbf{S}} + \sqrt{\mathbf{S}^{T}\mathbf{B}\mathbf{S}}}$
- $\mathbf{M}^{\mathrm{TS-BFGS}} = \mathbf{Y}\mathbf{Y}^{T} + |\mathbf{B}|\,\mathbf{S}\mathbf{S}^{T}\,|\mathbf{B}|$

$|\mathbf{B}| = \sum_i \left|\tilde{\lambda}_i\right| \tilde{\mathbf{v}}_i \tilde{\mathbf{v}}_i^{T}$, where $(\tilde{\lambda}_i, \tilde{\mathbf{v}}_i)$ are the eigenpairs of $\mathbf{B}$.

Benchmark systems

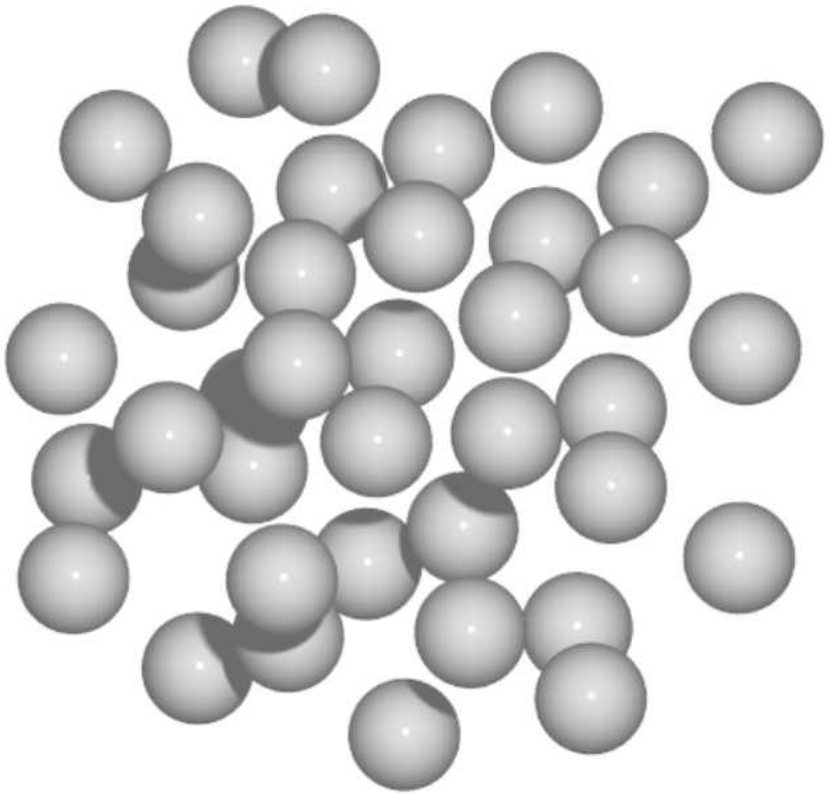

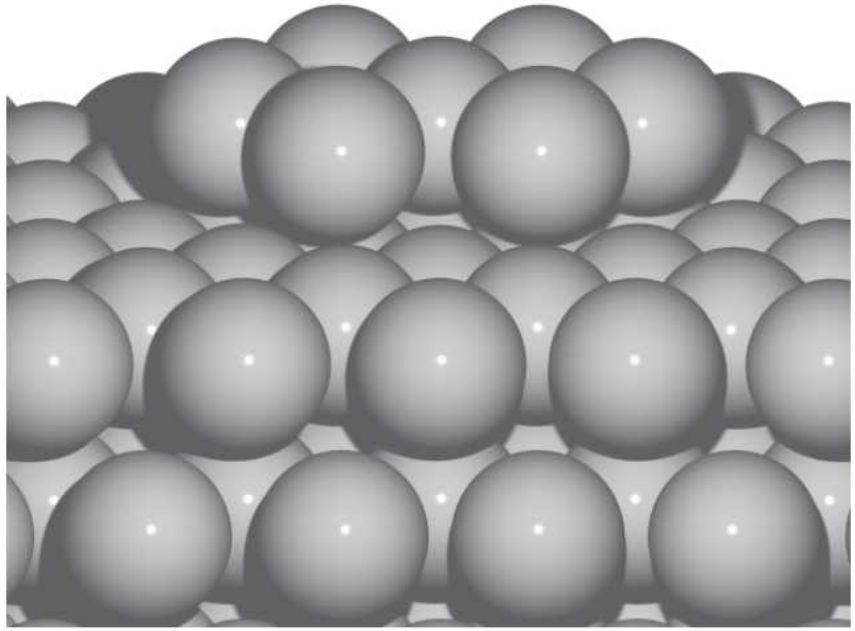

FOSP refinement benchmarks

Code	mean(n_{grad})	min(n_{grad})	max(n_{grad})
Sella	70	24	159
Optim	145	57	565
Pele	192	59	1488

Table: LJ38 optbench.org FOSP refinement benchmark.

Code	mean(n_{grad})	min(n_{grad})	max(n_{grad})
Sella	53	31	108
Optim	71	43	143
Pele	88	52	198

Table: Pt-heptamer island optbench.org FOSP refinement benchmark.

The diagonalization convergence criterion

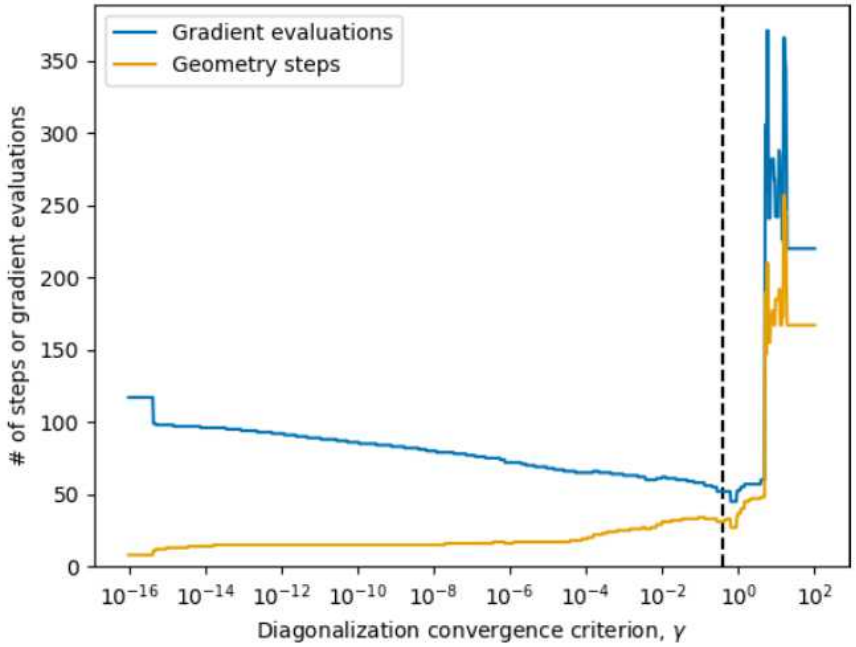

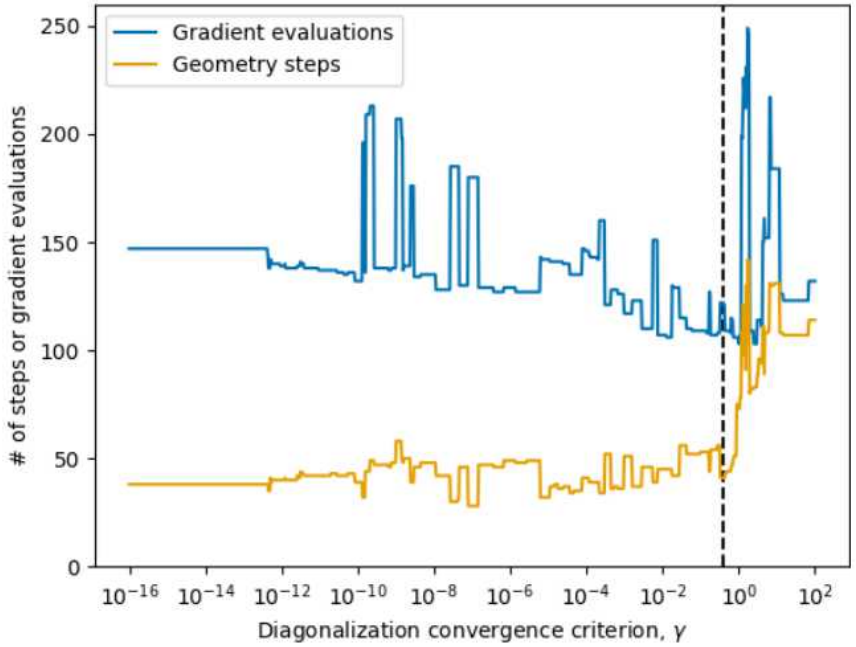

Sphingomyelin: Cartesian optimization

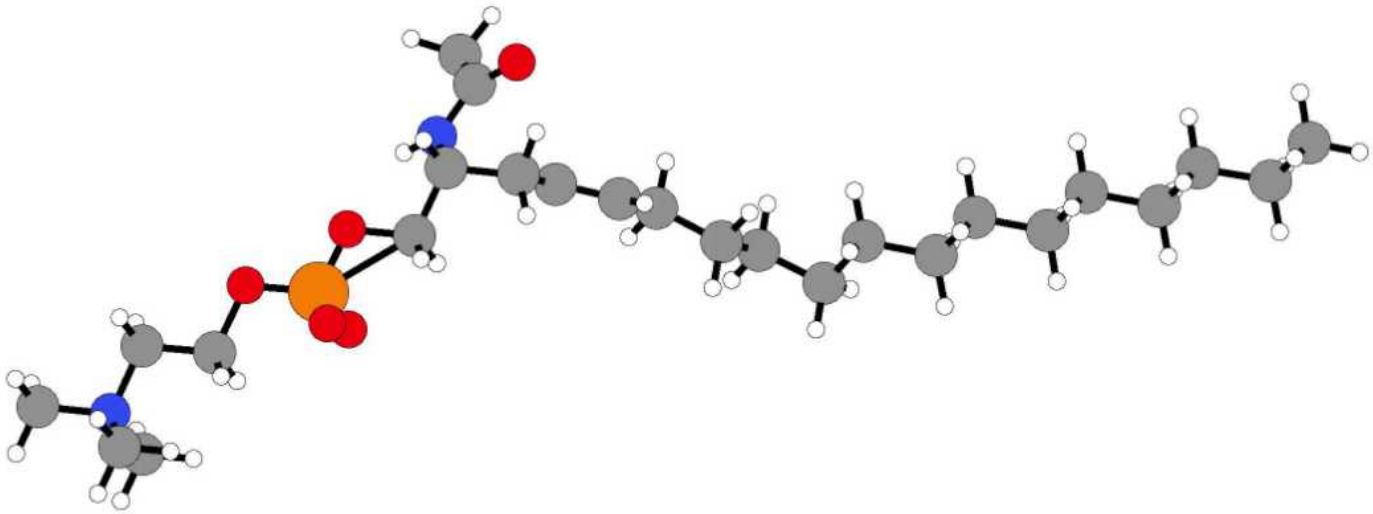

Sphingomyelin: Internal optimization

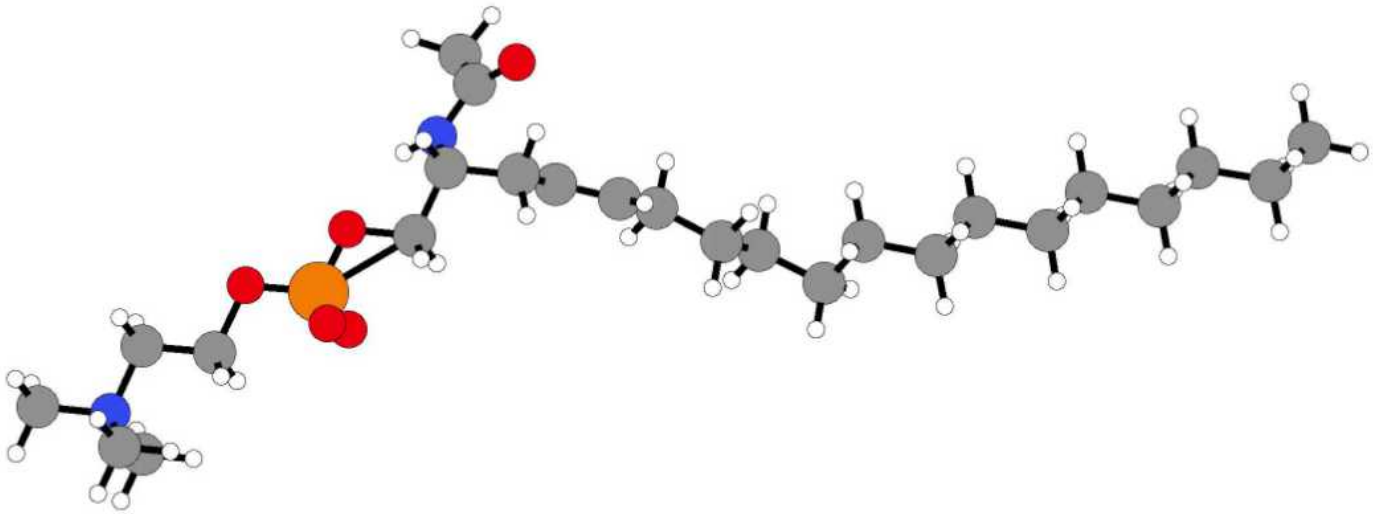

Sphingomyelin: Internal optimization (slower)

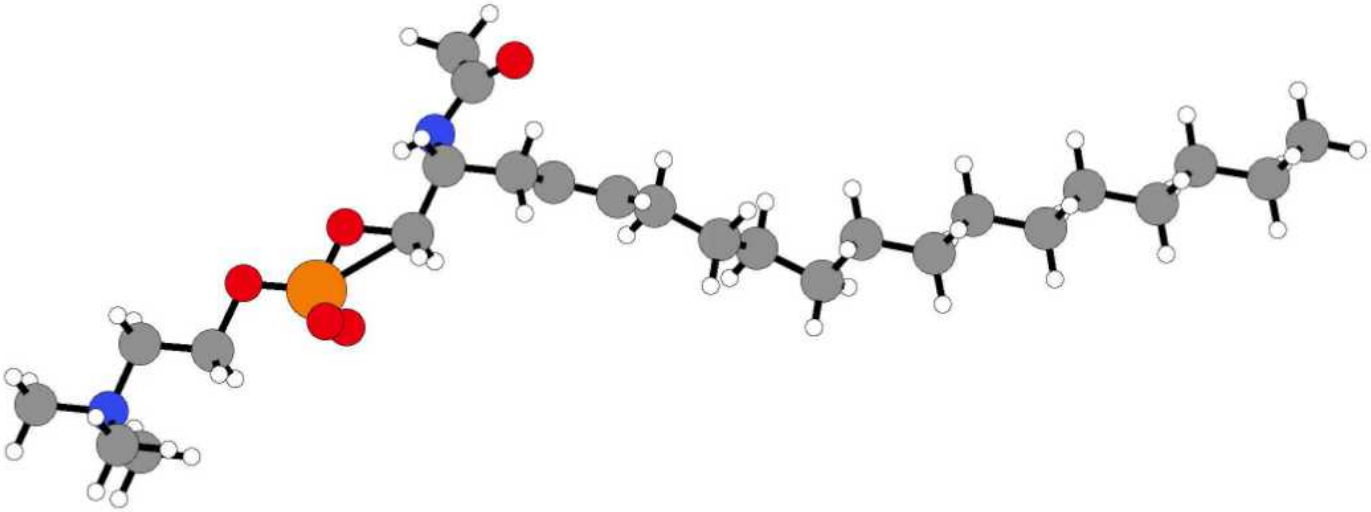

Types of internal coordinates

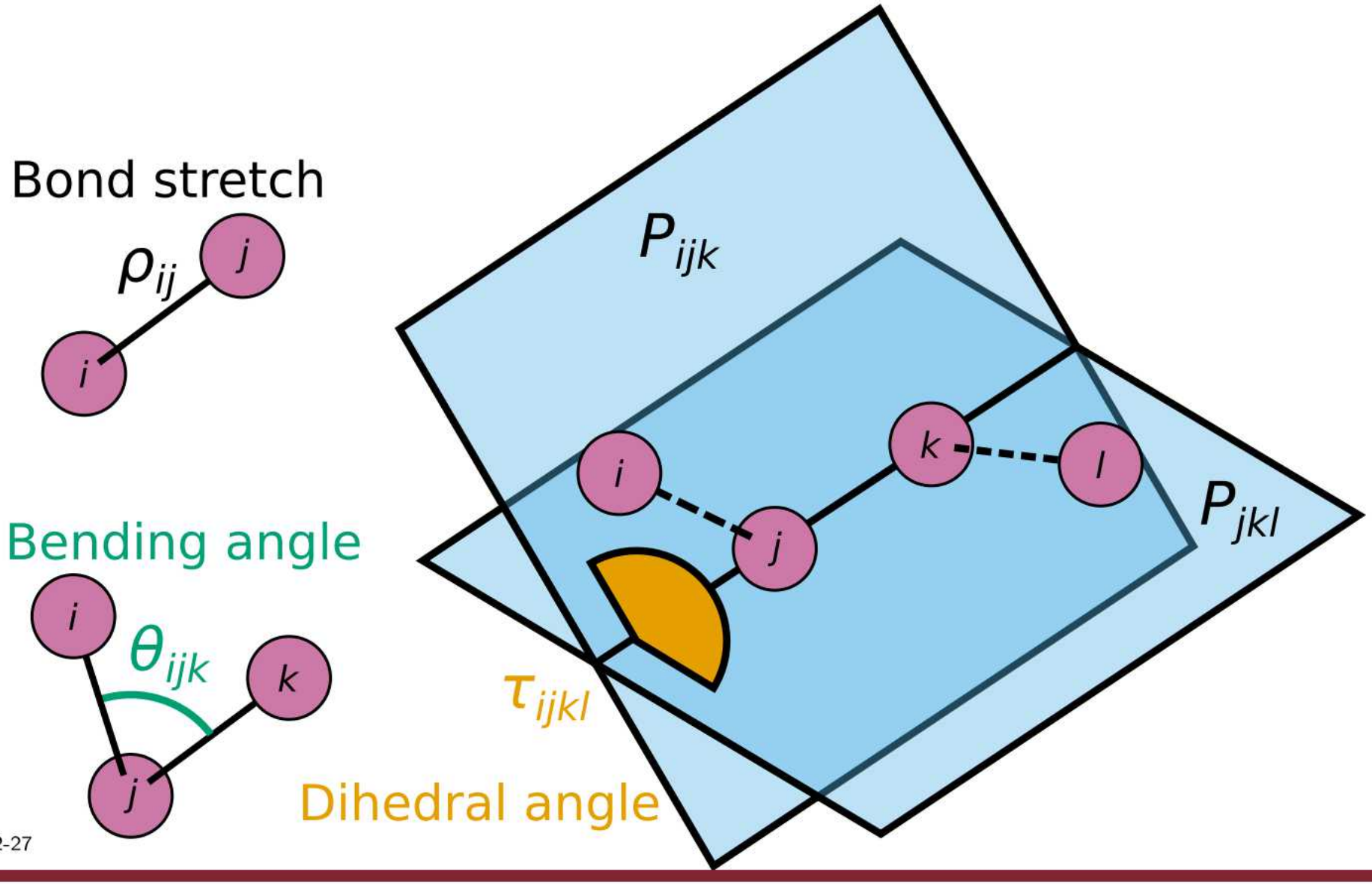

What does internal coordinate optimization mean?

Internal coordinates are defined by a function $\mathbf{q} : \mathbb{R}^{3n} \mapsto \mathbb{R}^k$, $k \geq 3n - 6$.
Quadratic approximation in Cartesian coordinates:

$$\epsilon(\mathbf{x}_0 + \mathbf{s}) \approx \epsilon(\mathbf{x}_0) + \mathbf{s}^T \left.\frac{d\epsilon}{d\mathbf{x}}\right|_{\mathbf{x}_0} + \frac{1}{2}\mathbf{s}^T \left.\frac{d^2\epsilon}{d\mathbf{x}^2}\right|_{\mathbf{x}_0} \mathbf{s}$$

Quadratic approximation in internal coordinates:

$$\epsilon(\mathbf{q}_0 + \mathbf{t}) \approx \epsilon(\mathbf{q}_0) + \mathbf{t}^T \left.\frac{d\epsilon}{d\mathbf{q}}\right|_{\mathbf{q}_0} + \frac{1}{2}\mathbf{t}^T \left.\frac{d^2\epsilon}{d\mathbf{q}^2}\right|_{\mathbf{q}_0} \mathbf{t}$$

These are not the same thing! For example:

$$\frac{d^2\epsilon}{d\mathbf{q}^2} = \left(\frac{d\mathbf{x}}{d\mathbf{q}}\right)^T \left(\frac{d^2\epsilon}{d\mathbf{x}^2} - \frac{d\epsilon}{d\mathbf{q}}\frac{d^2\mathbf{q}}{d\mathbf{x}^2}\right)\left(\frac{d\mathbf{x}}{d\mathbf{q}}\right)$$

Steps in internal coordinate space

How do we find the next set of coordinates?

Internal coordinate space is generally both *redundant* and *curved*, so $\mathbf{q} + \mathbf{t}$ may not exist!

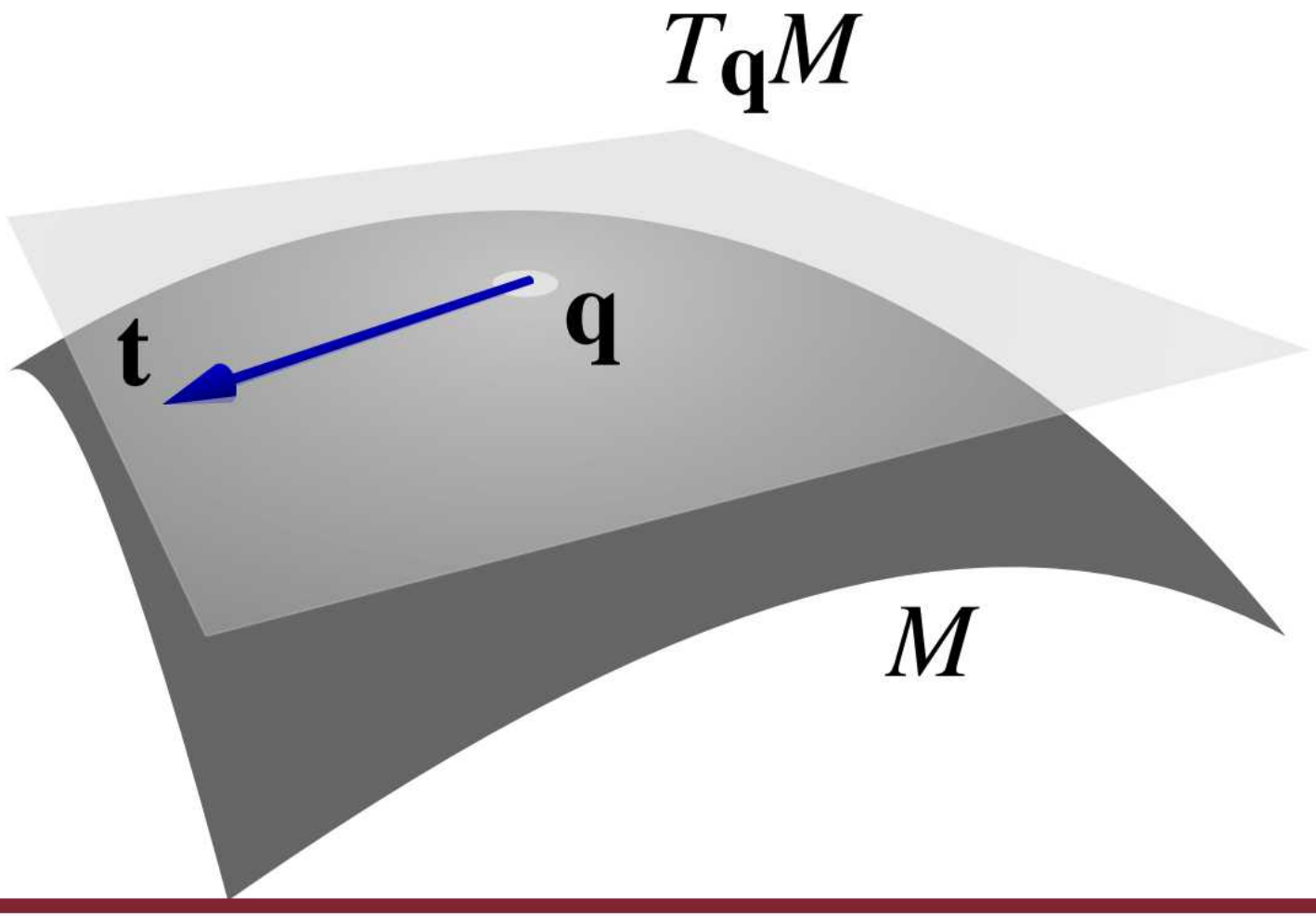

Standard approach

Repeat until convergence: $\mathbf{x}_{k+1} = \mathbf{x}_k + \left.\frac{d\mathbf{x}}{d\mathbf{q}}\right|_{\mathbf{x}_k} (\mathbf{q} + \mathbf{t} - \mathbf{q}(\mathbf{x}_k))$.

This process sometimes *diverges*!

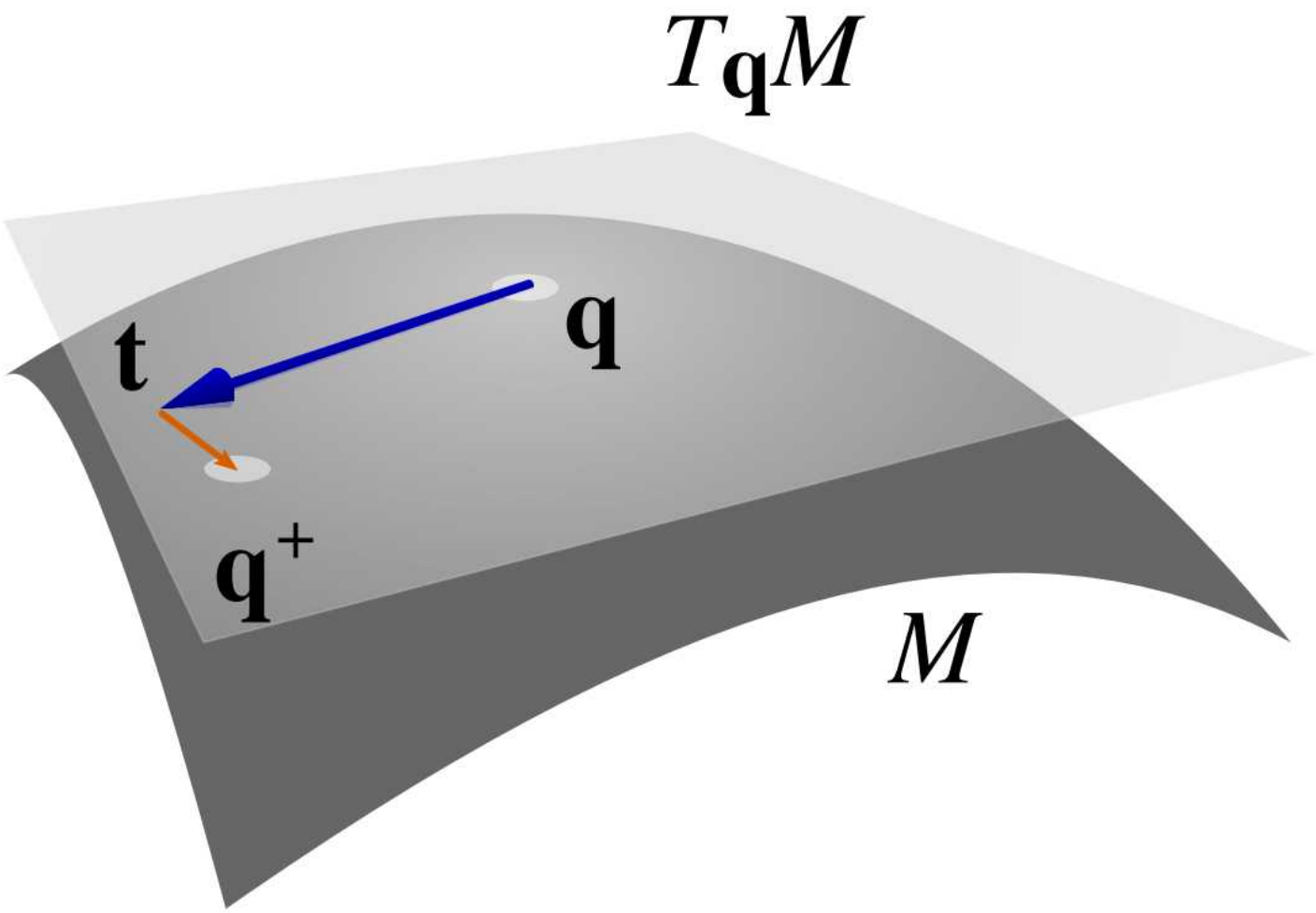

Geodesics

For any point $\mathbf{q} \in M$ and for any vector $\mathbf{t} \in T_{\mathbf{q}}M$ (the tangent space to M at $\mathbf{q}$), there exists a unique geodesic $\mathbf{u}(\tau)$ such that $\mathbf{u}(0) = \mathbf{q}$ and $\dot{\mathbf{u}}(0) = \mathbf{t}$.

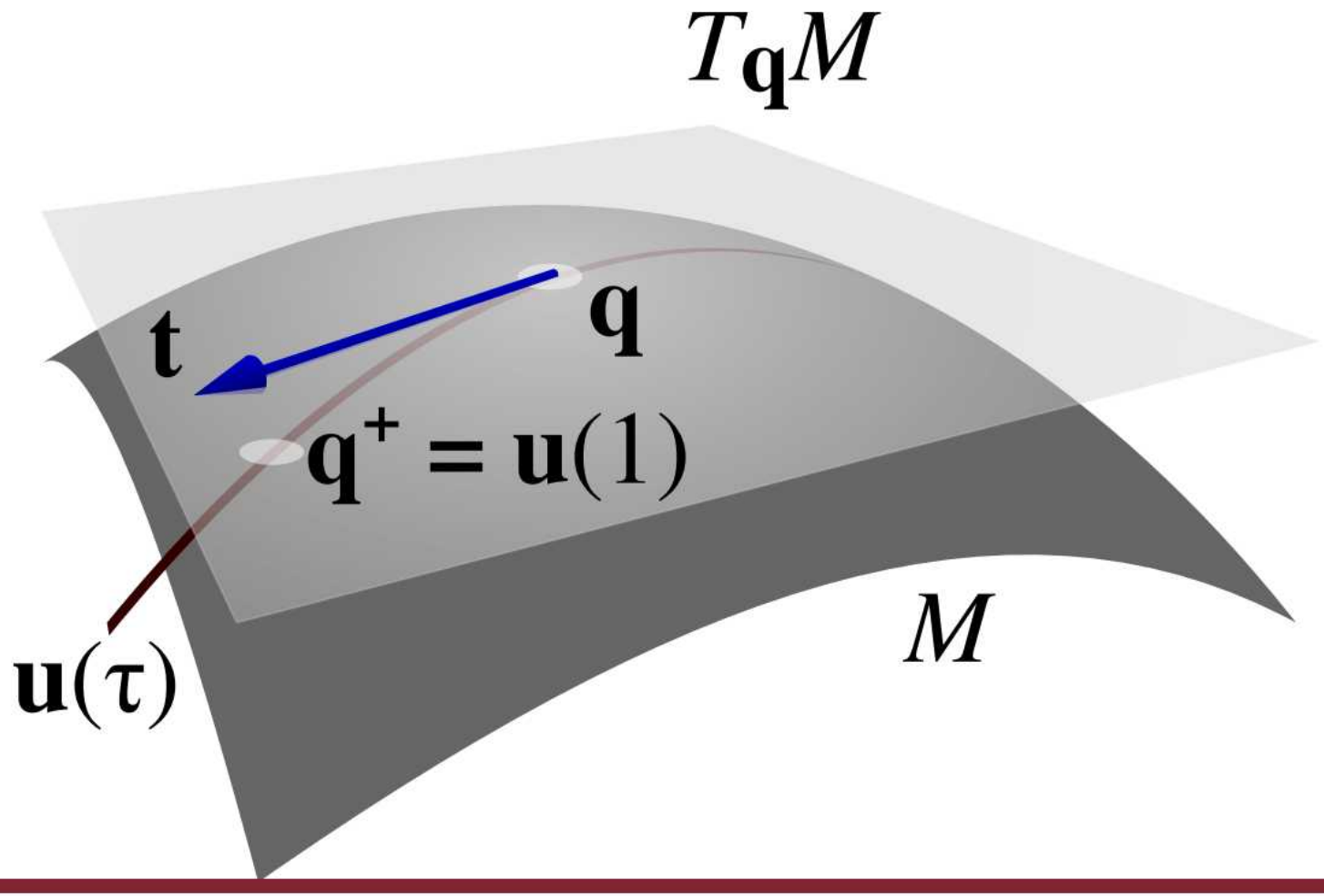

Finding the geodesic

The next structure $\mathbf{u}(1)$ is determined by the initial values $\mathbf{u}(0) = \mathbf{q}$ and $\dot{\mathbf{u}}(0) = \mathbf{t}$. But we still can't easily find the *Cartesian coordinates* that correspond to $\mathbf{u}(1)$.
Solution: Transform the differential equation into Cartesian coordinates

$$\mathbf{u}(0) = \mathbf{q} \qquad \mathbf{y}(0) = \mathbf{x}$$

$$\dot{\mathbf{u}}(0) = \mathbf{t} \qquad \dot{\mathbf{y}}(0) = \left[\left. \frac{d\mathbf{x}}{d\mathbf{q}} \right|_{\mathbf{y}(0)} \right] \mathbf{t}$$

$$\ddot{\mathbf{u}}(\tau) = \mathbf{0} \qquad \ddot{\mathbf{y}}(\tau) = -\left[\left. \frac{d\mathbf{x}}{d\mathbf{q}} \right|_{\mathbf{y}(\tau)} \right] \left[\left. \frac{d^2\mathbf{q}}{d\mathbf{x}^2} \right|_{\mathbf{y}(\tau)} \right] \dot{\mathbf{y}}(\tau)\dot{\mathbf{y}}(\tau)$$

$\dot{\mathbf{u}}(\tau)$ stays (mostly) constant even though $\dot{\mathbf{y}}(\tau) = \left[\left. \frac{d\mathbf{x}}{d\mathbf{q}} \right|_{\mathbf{y}(\tau)} \right] \dot{\mathbf{u}}(\tau)$ does not.

Bond stretches: Naive approach

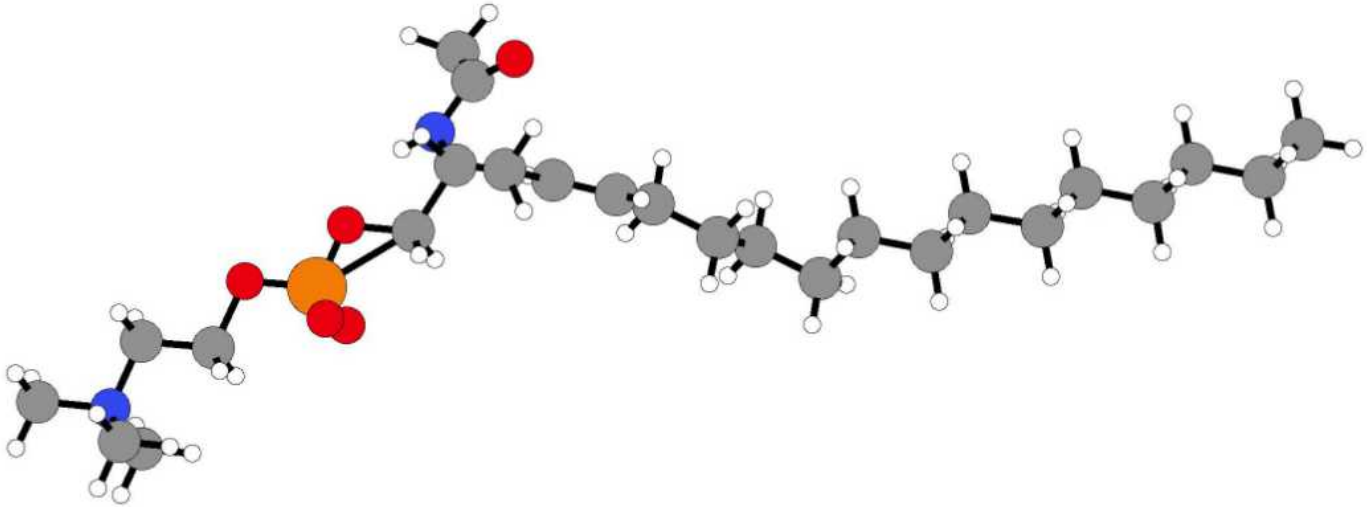

Bond stretches: Internal coordinate optimization

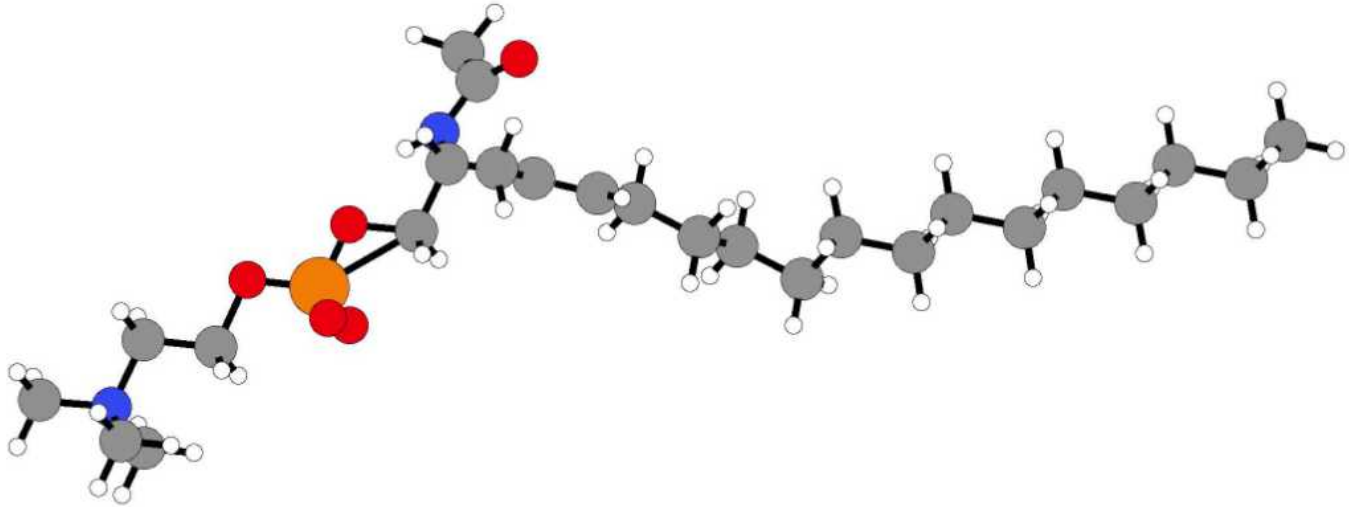

Bending angles: Naive approach

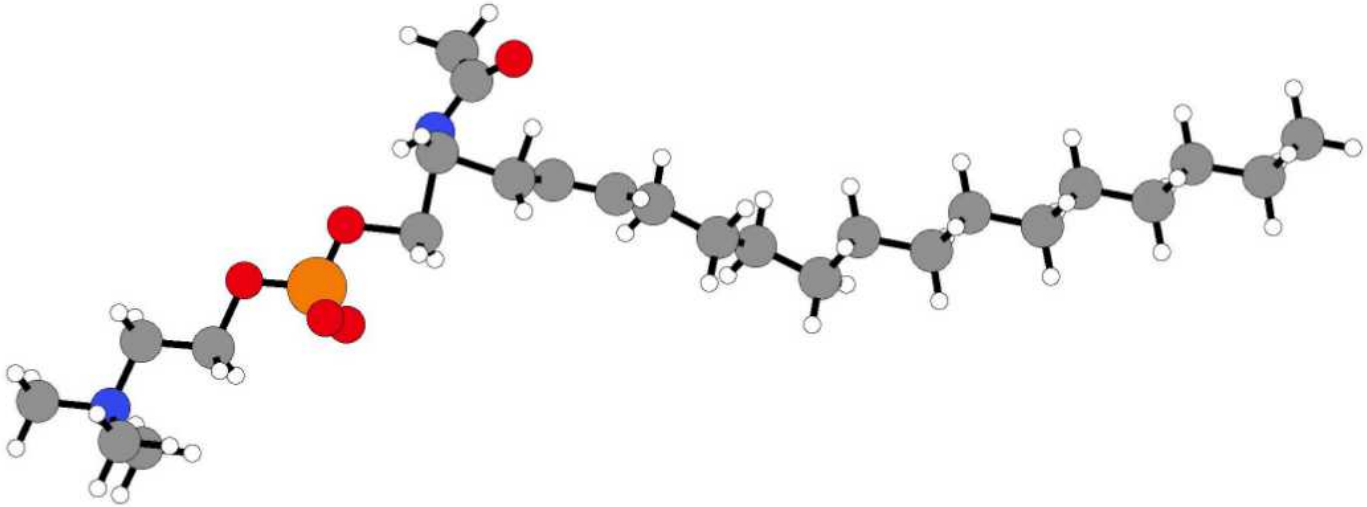

Bending angles: Internal coordinate optimization

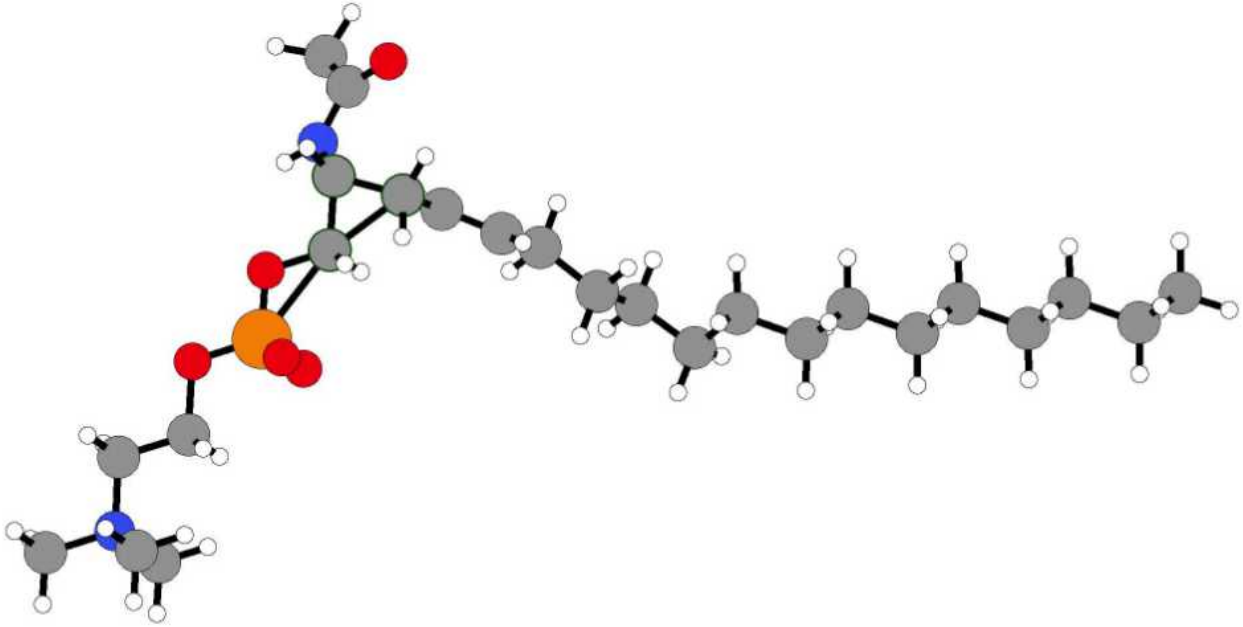

Dihedral angles: Naive approach

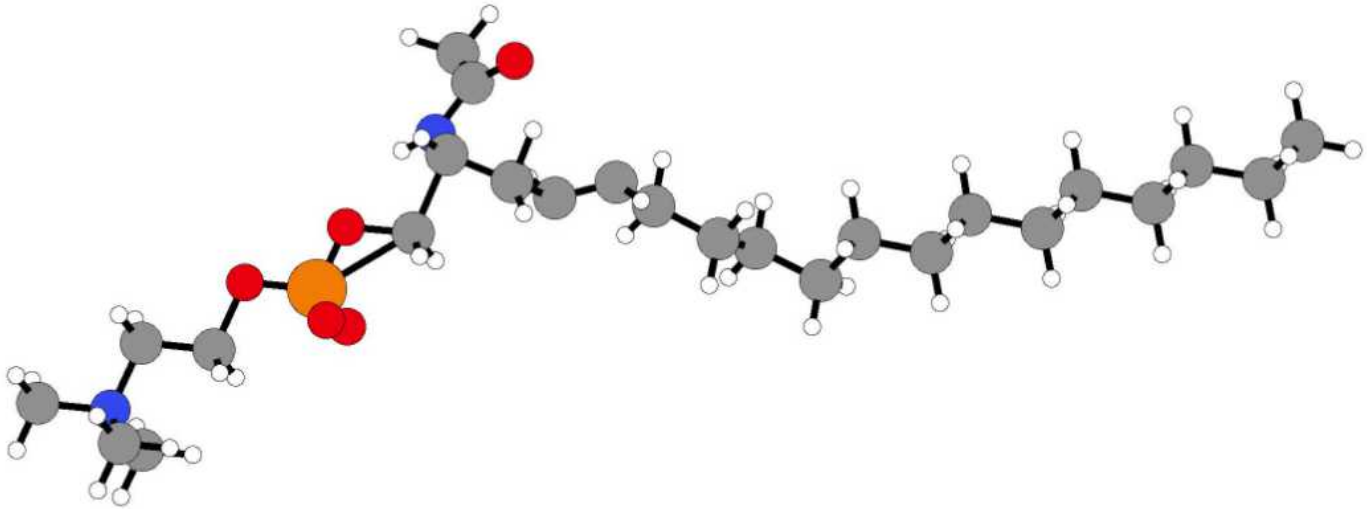

Dihedral angles: Internal coordinate optimization

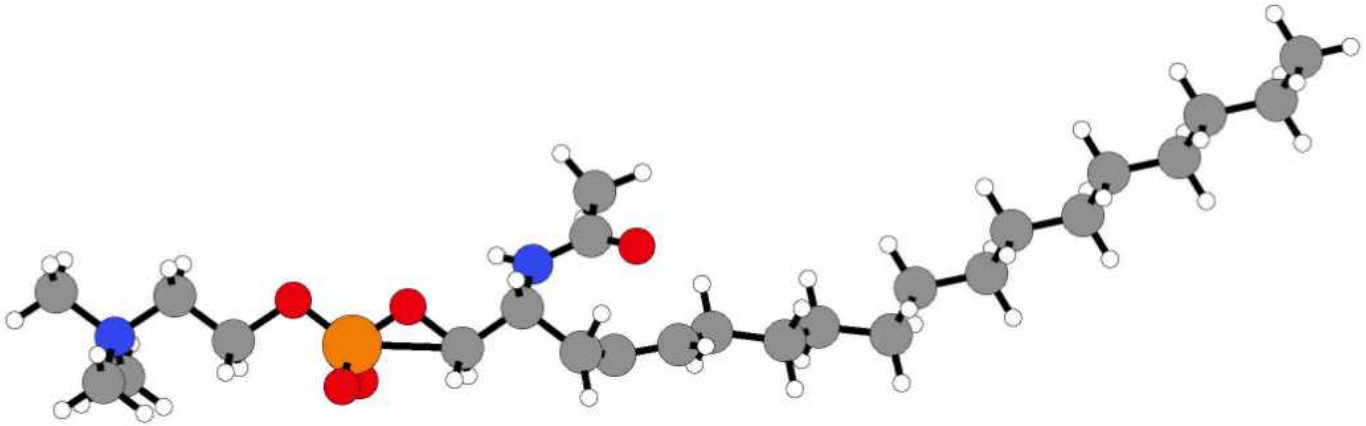

Internal coordinate singularities

The internal coordinate Jacobian can have discontinuities:

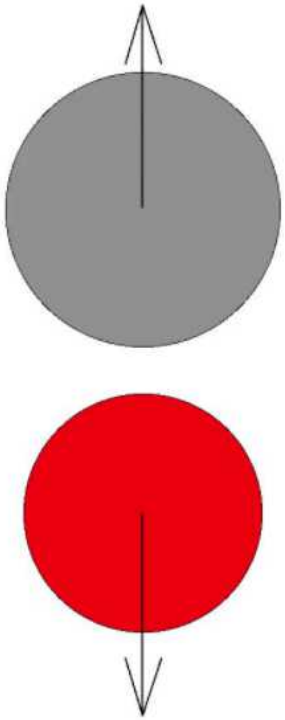

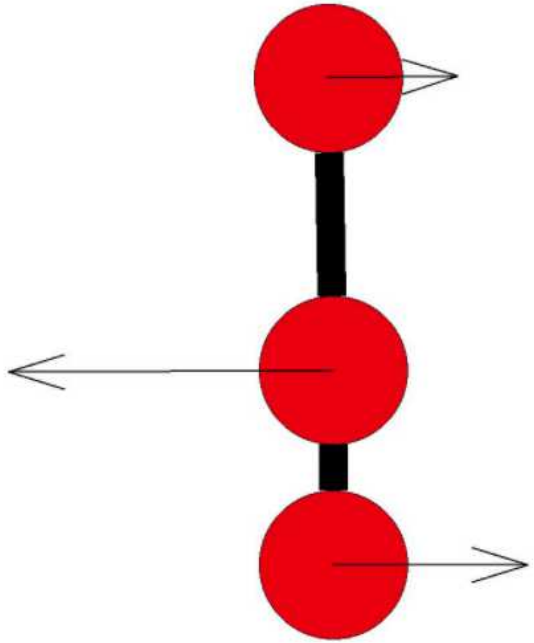

Internal coordinate singularities

The internal coordinate Jacobian can have discontinuities *or singularities*:

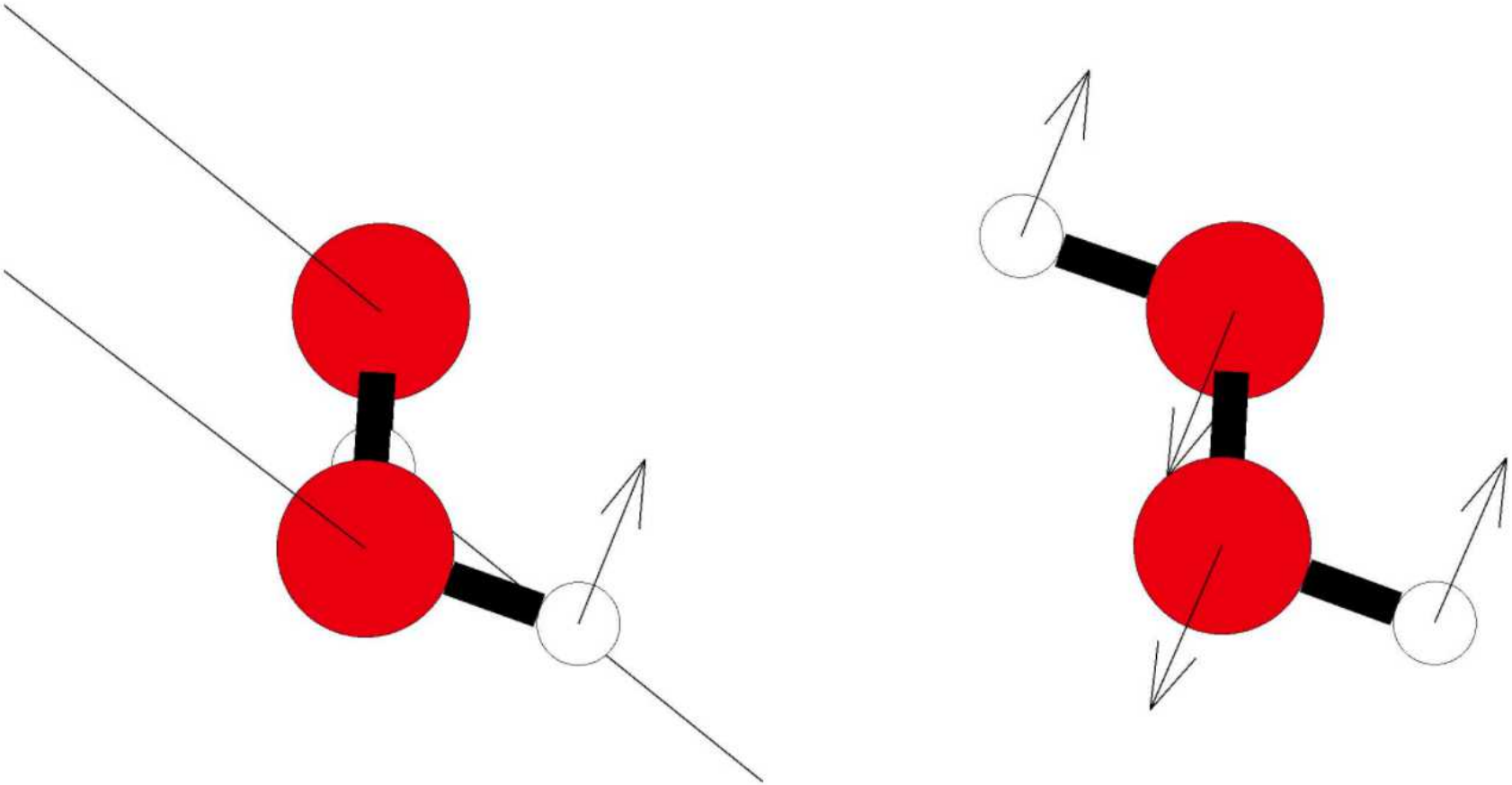

Dummy atoms

Dummy atoms are “fake” atoms which are used to construct more well-behaved internal coordinates.

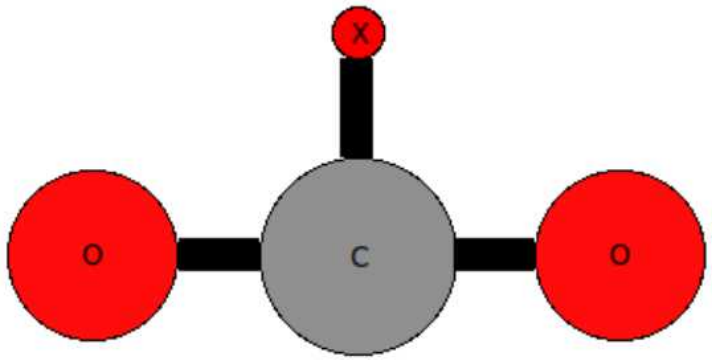

To counteract the dimensionality increase, constraints can be added.

Constrained optimization

Constrained minimization problem: Minimize $\epsilon(\mathbf{q})$ subject to $\mathbf{c}(\mathbf{q}) = \mathbf{0}$. Solutions are minima of the Lagrangian:

$$\mathcal{L}(\mathbf{q}, \mathbf{w}) = \epsilon(\mathbf{q}) - \mathbf{w}^T \mathbf{c}(\mathbf{q})$$

To make this tractable, we define a series of iterates $\mathbf{q}^+ = \mathbf{q} + \mathbf{t}$ obtained by iteratively minimizing the quadratic function:

$$\mathbf{t}^T \left(\frac{d\epsilon}{d\mathbf{q}} \right) + \frac{1}{2} \mathbf{t}^T \left(\frac{d^2 \mathcal{L}}{d\mathbf{q}^2} \right) \mathbf{t}$$

subject to the linearized constraint equation:

$$\mathbf{c}(\mathbf{q}) + \left(\frac{d\mathbf{c}}{d\mathbf{q}} \right) \mathbf{t} = \mathbf{0}.$$

This is known as Sequential Quadratic Programming.

Null-space SQP

Define full column rank matrices $\mathbf{N}$, $\mathbf{P}$, and $\mathbf{Q}$ where:

- $\mathbf{N}$ spans the *normal space* at the current point
- $\mathbf{P}$ is orthogonal to $\mathbf{N}$ and spans the columns of $\frac{d\mathbf{c}}{d\mathbf{q}}$
- $\mathbf{Q}$ is orthogonal to both $\mathbf{N}$ and $\mathbf{P}$.

Then we can write $\mathbf{t} = \mathbf{P}\mathbf{t}_P + \mathbf{Q}\mathbf{t}_Q$, where $\mathbf{t}_P$ is obtained by solving (in the least squares sense)

$$\left(\frac{d\mathbf{c}}{d\mathbf{q}}\right)\mathbf{P}\mathbf{t}_P = -\mathbf{c},$$

and $\mathbf{t}_Q$ is obtained by minimizing the *projected* quadratic approximation:

$$\mathbf{t}_Q^T\mathbf{Q}^T\left(\frac{d\epsilon}{d\mathbf{q}} + \left(\frac{d^2\epsilon}{d\mathbf{q}^2}\right)\mathbf{P}\mathbf{t}_P\right) + \frac{1}{2}\mathbf{t}_Q^T\mathbf{Q}^T\left(\frac{d^2\mathcal{L}}{d\mathbf{q}^2}\right)\mathbf{Q}\mathbf{t}_Q$$

Hessian of the Lagrangian

$$\frac{d^2\mathcal{L}}{d\mathbf{q}^2} = \frac{d^2\epsilon}{d\mathbf{q}^2} - \mathbf{w}^T\left(\frac{d^2\mathbf{c}}{d\mathbf{q}^2}\right)$$
$$= \frac{d^2\epsilon}{d\mathbf{q}^2} - \mathbf{w}^T\left(\frac{d\mathbf{x}}{d\mathbf{q}}\right)^T\left(\frac{d^2\mathbf{c}}{d\mathbf{x}^2} - \left(\frac{d\mathbf{c}}{d\mathbf{q}}\right)\left(\frac{d^2\mathbf{q}}{d\mathbf{x}^2}\right)\right)\left(\frac{d\mathbf{x}}{d\mathbf{q}}\right)$$

This requires the second derivative of both **c** and **q** with respect to the Cartesian positions **x**.
At convergence, **w** satisfies the relation

$$\left(\frac{d\mathbf{c}}{d\mathbf{q}}\right)^T\mathbf{w} = \frac{d\epsilon}{d\mathbf{q}}.$$

We define **w** at intermediate steps by solving this equation in the least squares sense.

Preliminary results: minimization[7]

Sella	DL-FIND		Sella	DL-FIND	
RFO	GPR	L-BFGS	RFO	GPR	L-BFGS
11	15	19	52	16	23
14	16	26	11	12	13
25	18	46	15	15	80
9	12	14	28	109	104
24	29	31	14	29	39
20	26	27	17	13	26
26	68	62	15	22	35
23	38	42	20	19	22
48	77	83	11	19	22
11	13	15	16	14	19
10	34	37	18	19	23
13	15	23	184	25	29
11	14	19			

[7] Denzel, A.; Kästner, J. *The Journal of Chemical Physics* **2018**, *148*, 094114

Preliminary results: saddle point refinement[8]

Sella	DL-FIND			Sella	DL-FIND		
P-RFO	GPRTS	dimer	P-RFO	P-RFO	GPRTS	dimer	P-RFO
10	18	39	30	20	34	76	80
12	14	34	35	18	-	59	-
13	16	31	127	23	31	67	79
23	36	152	66	22	34	83	130
19	25	59	85	29	101	288	232
26	47	106	175	17	22	69	44
51	41	100	507	19	24	211	142
15	28	63	83	22	100	-	55
25	47	171	-	12	18	44	174
68	25	224	151	15	16	38	56
22	49	-	71	28	19	58	114
19	22	53	68	17	23	45	59
27	31	88	73				

[8] Denzel, A.; Kästner, J. *Journal of Chemical Theory and Computation* **2018**, *14*, 5777–5786

Acknowledgments

This work was supported by the U.S. Department of Energy, Office of Science, Basic Energy Sciences, Chemical Sciences, Geosciences and Biosciences Division, as part of the Computational Chemistry Sciences Program (Award Number: 0000232253).

References I

[1] Gao, C. W.; Allen, J. W.; Green, W. H.; West, R. H. *Computer Physics Communications* **2016**, *203*, 212–225.

[2] Cao, A.; Veser, G. *Nature Materials* **2010**, *9*, 75–81.

[3] Divi, S.; Chatterjee, A. *RSC Advances* **2018**, *8*, 10409–10424.

[4] Lonie, D. C.; Zurek, E. *Computer Physics Communications* **2012**, *183*, 690–697.

[5] Hermes, E. D.; Sargsyan, K.; Najm, H. N.; Zádor, J. *Journal of Chemical Theory and Computation* **2019**, *15*, 6536–6549.

[6] Schlegel, H. B. *Journal of Computational Chemistry* **1982**, *3*, 214–218.

[7] Denzel, A.; Kästner, J. *The Journal of Chemical Physics* **2018**, *148*, 094114.

[8] Denzel, A.; Kästner, J. *Journal of Chemical Theory and Computation* **2018**, *14*, 5777–5786.